Published in final edited form as:
Cell Microbiol. 2012 July ; 14(7): 1051–1070. doi:10.1111/j.1462-5822.2012.01778.x.

The enteropathogenic *E. coli* effector EspH promotes actin pedestal formation and elongation via WASP-interacting protein (WIP)

Alexander R. C. Wong, **Benoit Raymond**, **James W. Collins**, **Valerie F. Crepin**, and **Gad Frankel***
Centre for Molecular Microbiology and Infection, Division of Cell and Molecular Biology, Imperial College London, London SW7 2AZ, UK

Summary

Enteropathogenic and enterohaemorrhagic *Escherichia coli* (EPEC and EHEC) are diarrheagenic pathogens that colonize the gut mucosa via attaching-and-effacing lesion formation. EPEC and EHEC utilize a type III secretion system (T3SS) to translocate effector proteins that subvert host cell signalling to sustain colonization and multiplication. EspH, a T3SS effector that modulates actin dynamics, was implicated in the elongation of the EHEC actin pedestals. In this study we found that EspH is necessary for both efficient pedestal formation and pedestal elongation during EPEC infection. We report that EspH induces actin polymerization at the bacterial attachment sites independently of the Tir tyrosine residues Y474 and Y454, which are implicated in binding Nck and IRSp53/ITRKS respectively. Moreover, EspH promotes recruitment of neural Wiskott–Aldrich syndrome protein (N-WASP) and the Arp2/3 complex to the bacterial attachment site, in a mechanism involving the C-terminus of Tir and the WH1 domain of N-WASP. Dominant negative of WASP-interacting protein (WIP), which binds the N-WASP WH1 domain, diminished EspH-mediated actin polymerization. This study implicates WIP in EPEC-mediated actin polymerization and pedestal elongation and represents the first instance whereby N-WASP is efficiently recruited to the EPEC attachment sites independently of the Tir:Nck and Tir:IRTKS/IRSp53 pathways. Our study reveals the intricacies of Tir and EspH-mediated actin signalling pathways that comprise of distinct, convergent and synergistic signalling cascades.

Introduction

The actin cytoskeleton plays a critical role in many cellular processes, including cell morphology, migration, cytokinesis and apoptosis. As a result, many bacterial pathogens hijack the host actin machinery to enhance colonization and dissemination. Enteropathogenic *Escherichia coli* (EPEC), enterohaemorrhagic *E. coli* (EHEC) (Nataro and Kaper, 1998; Wong *et al*., 2011) and the closely related mouse pathogen *Citrobacter rodentium* (Mundy *et al*., 2005) belong to a group of mainly extracellular diarrheagenic pathogens that colonize the gut epithelium by attaching-and-effacing (A/E) lesions (Frankel

*For correspondence. g.frankel@imperial.ac.uk; Tel. (+44) 20 75945253; Fax (+44) 20 75943069.

Europe PMC Funders Author Manuscripts

and Phillips, 2008). The A/E histopathology is characterized by effacement of the brush border microvilli, intimate bacterial adherence to the enterocyte apical plasma membrane, and the accumulation of polymerized actin beneath the attached bacteria (Knutton *et al.*, 1987). In cultured cells, EPEC-induced actin polymerization leads to formation of actin-rich pedestals.

Formation of A/E legions *in vivo* and actin pedestals *in vitro* is dependent on the outer membrane bacterial adhesin intimin (Jerse and Kaper, 1991) and the translocated intimin receptor (Tir) (Kenny *et al.*, 1997). Upon translocation, Tir is inserted into the plasma membrane in a hairpin loop topology, with cytoplasmic N- and C-termini and an extracellular middle loop which binds intimin (Kenny *et al.*, 1997; Hartland *et al.*, 1999). Intimin : Tir interaction results in Tir clustering and the initiation of downstream signalling events that lead to the formation of the actin-rich pedestals (Frankel and Phillips, 2008).

EPEC-induced actin polymerization is attributed to the C-terminus of Tir. In the prototypical EPEC strain E2348/69, phosphorylation of the Tir tyrosine residue 474 (Y474) by host cell tyrosine kinases (Phillips *et al.*, 2004; Swimm *et al.*, 2004; Bommarius *et al.*, 2007) generates a binding site for the mammalian cell adaptor protein Nck, which then recruits and activates the neural Wiskott–Aldrich syndrome protein (N-WASP) leading to stimulation of strong Arp2/3-mediated actin polymerization (Kenny, 1999; Gruenheid *et al.*, 2001). In addition, Tir can also promote weak Nck-independent actin polymerization through tyrosine residue Y454 that forms part of a conserved Asn-Pro-Tyr (NPY) motif (Campellone and Leong, 2005; Brady *et al.*, 2007). The NPY motif recruits the insulin receptor tyrosine kinase substrate p53 (IRSp53) family of proteins IRTKS (Vingadassalom *et al.*, 2009) and IRSp53 (Weiss *et al.*, 2009) in EPEC, leading to activation of yet unknown downstream actin polymerization signalling pathways. Importantly, we have recently reported that although not affecting *C. rodentium* bacterial load and A/E lesion formation *in vivo*, Tir residues Y451 and Y471, and by extension Tir:Nck and Tir:IRTKS/IRSp53 signalling pathways, provide the bacterium with competitive edge and higher fitness *in vivo* (Crepin *et al.*, 2009).

N-WASP consists of several domains. The C-terminal verprolin-central-acidic (VCA) domain binds and activates the Arp2/3 complex (Rohatgi *et al.*, 1999), while the WASP-homology 1 (WH1), Basic (B), GTPase-binding domain (GBD) and proline-rich domain (PRD) integrate multiple upstream signals to regulate the localization and activation of the protein (Takenawa and Suetsugu, 2007; Padrick and Rosen, 2010). Although Nck binds directly to N-WASP via the PRD domain (Anton *et al.*, 1998; Rohatgi *et al.*, 2001), the PRD domain is dispensable for pedestal formation. Instead, the WH1 domain of N-WASP is required for EPEC pedestal formation (Lommel *et al.*, 2001). The WASP-interacting protein (WIP) family, which comprise WIP (Ramesh *et al.*, 1997), CR16 (Weiler *et al.*, 1996; Ho *et al.*, 2001) and WICH/WIRE (Aspenstrom, 2002; Kato *et al.*, 2002), are known interacting partners of the WH1 domain of WASP/N-WASP. WIP binds WH1 domain via its C-terminus region, termed the WASP-binding domain (WBD) (Volkman *et al.*, 2002; Peterson *et al.*, 2007).

EspH is a T3SS effector that was implicated in modulating actin dynamics. Deletion of *espH* in EHEC resulted in short pedestals, while overexpression of EspH led to pedestal

elongation (Tu *et al.*, 2003). Although EspH is not required for A/E lesion formation, several studies have indicated its importance in bacterial adherence and colonization (Ritchie and Waldor, 2005; Shaw *et al.*, 2005). Recently, Dong *et al.* (2010) reported that EspH is a RhoGEF inhibitor that acts by competitively binding to the tandem Dbl-homology and pleckstrin-homology (DH-PH) domains of Dbl-family mammalian RhoGEFs (Dong *et al.*, 2010). The aim of this study is to further characterize the role EspH plays in modulating actin dynamics during EPEC infection.

Results

EspH promotes both pedestal formation and pedestal elongation during EPEC infection

To assess the role of EspH in the kinetics of EPEC-induced pedestal formation, Swiss 3T3 fibroblasts were infected with wild-type E2348/69, E2348/69Δ*espH* or E2348/69Δ*espH* complemented with EspH. Microcolonies (5 or more bacteria) associated with pedestals were then enumerated by immunofluorescence microscopy at time intervals of 10, 20, 30, 45 or 90 min post infection. Actin pedestals were observed in 88.8 ± 5.8% of E2348/69 microcolonies at 30 min post infection (Fig. S1A). In contrast, only 41.7 ± 5.5% of microcolonies were associated with pedestals in the *espH* mutant. In addition, at 90 min, pedestals formed by the E2348/69Δ*espH* mutant were markedly shorter than those observed in the other strains (Fig. S1B). Pedestals formed by the E2348/69Δ*espH* mutant did not appear elongated even after 2 h of infection (data not shown). These results confirm that EspH is involved in promoting the formation and elongation of EPEC actin pedestals (Tu *et al.*, 2003).

EspH triggers actin signalling pathways independently of Tir tyrosine residues Y454 and Y474

As EspH modulates the length of the EPEC actin pedestals, we hypothesized that it could amplify one of the Tir actin signalling pathways. We constructed E2348/69 chromosomally expressing Tir_{Y454A} (mutated at the IRSp53/IRTKS binding site), Tir_{Y474A} (mutated at the Nck-binding site) and $Tir_{Y454A/Y474A}$ (double mutant), using the lambda red mutagenesis strategy (Datsenko and Wanner, 2000; Crepin *et al.*, 2009) involving insertion of a kanamycin cassette in the *tir-cesT* intergenic region (Fig. 1A). A control mock mutant was also generated with the insertion of the kanamycin cassette, but without modification to the *tir* coding sequence (Tir_{WT}). We first assessed the ability of these Tir mutants to translocate Tir and induce actin polymerization in infected Swiss 3T3 fibroblasts. Tir_{WT} and Tir_{Y454A} localized under adherent bacteria and formed actin pedestals (Figs 1B and S2), while Tir_{Y474A} and $Tir_{Y454A/Y474A}$ were detected underneath E2348/69 but did not trigger actin polymerization (Figs 1B and S2). Neither Tir nor actin polymerization was observed under the attached E2348/69Δ*tir* control strain.

We then expressed HA-tagged EspH in the same strains and assessed its impact on actin polymerization. Unexpectedly, EspH triggered localized actin polymerization in 38.5 ± 10.6% and 38.5 ± 10.9% of adherent E2348/69 expressing HA-EspH and Tir_{Y474A} or $Tir_{Y454A/Y474A}$ (Fig. 1B and C; Fig. S2). However, EspH-mediated actin polymerization was different from that formed by E2349/69 expressing Tir_{WT}, as the microcolonies were

surrounded by an actin 'coat', rather than associated with distinctive pedestals (Fig. 1B and C; Fig. S2). EspH was mainly localized to the membrane surrounding F-actin, and the plasma membrane of infected cells (Fig. 2C). In contrast, neither actin polymerization nor EspH was detected beneath adherent E2348/69Δ*tir* expressing HA-tagged EspH (Fig. 1C), indicating that recruitment of EspH and F-actin at the bacterial attachment site is Tir-dependent.

EspH promotes recruitment of N-WASP to the bacterial attachment site

To investigate the mechanism of actin polymerization triggered by E2348/69 coexpressing $Tir_{Y454A/Y474A}$ and EspH, we determined which actin promoting factors are recruited to the bacterial attachment site. Infection of Swiss 3T3 with E2348/69 expressing Tir_{WT} and $Tir_{Y454A/Y474A}$ was used as controls. Staining for N-WASP (Fig. 2A) and the Arp2 subunit of the Arp2/3 complex (Fig. 2B) 2 h post infection revealed that both proteins were accumulated underneath E2348/69 expressing Tir_{WT} and E2348/69 coexpressing $Tir_{Y454A/Y474A}$ and EspH. In contrast, only a few microcolonies of E2348/69 expressing $Tir_{Y454A/Y474A}$ were associated with N-WASP and the Arp2 subunit. we also investigated recruitment of IRSp53 and WAVE2 by transfection of their respective Myc-tagged constructs, but did not observe their recruitment to the bacterial attachment site, indicating that they are not required for EspH-mediated actin polymerization (Fig. S3). These results show that EspH promotes efficient recruitment of N-WASP and the Arp2/3 complex beneath EPEC microcolonies independently of the Tir tyrosine residues Y454 and Y474.

EspH promotes actin polymerization independently of Nck or Rho GTPases

In order to determine if Nck plays a role in EspH-mediated actin polymerization, we infected Nck-deficient ($Nck^{-/-}$) fibroblasts with E2348/69 expressing Tir_{WT} or $Tir_{Y454A/Y474A}$, with or without coexpression of EspH-HA. While E2348/69 coexpressing Tir_{WT} or $Tir_{Y454A/Y474A}$ and EspH triggered localized actin polymerization, E2348/69 expressing Tir_{WT} or $Tir_{Y454A/Y474A}$ alone did not (Fig. 3A). This result suggests that EspH mediates actin polymerization dependently of Nck.

To assess if the repression of Rho GTPases is involved in EspH-mediated actin polymerization, we performed siRNA knockdown of Cdc42, Rac1 and RhoA, and infected Swiss 3T3 fiboblasts with E2348/69 expressing $Tir_{Y454A/Y474A}$ with or without EspH. Specificity of RNAi-mediated silencing was assessed by Western blot (Fig. 3B). Quantification of EPEC microcolonies revealed no difference in actin-associated microcolonies compared with the scrambled siRNA control (Fig. 3B). This suggests that EspH-mediated actin polymerization is not a result of Rho GTPase inactivation.

EspH-mediated actin polymerization requires the C-terminus of Tir

We next determine which of the cytoplasmic Tir domains is involved in EspH-mediated N-WASP recruitment. Towards this end, we utilized a Tir complementation assay previously described (Campellone *et al.*, 2004a). We obtained an HA-tagged Tir derivative that has its N-terminus replaced with the transmembrane domain of the Newcastle Disease Virus HN protein, followed by the intimin-binding extracellular loop and C-terminus of Tir (HA-TirMC), and a similar construct but with a point Y474F mutation (HA-$TirMC_{Y474F}$) (kindly

provided by J. Leong). Using HA-TirMC as a template, we deleted the C-terminus tail and inserted the N-terminus of Tir before the HN transmembrane domain to generate HA-TirNM (Fig. 4A). Using GFP as negative control, we transfected the Tir derivatives into Swiss 3T3 fibroblasts; 30 h later the cells were infected for 2 h with E2348/69Δ*tir* expressing EspH. Triple staining of HA-tagged Tir, N-WASP, and intimin revealed that both HA-TirMC and HA-TirMC$_{Y474F}$, but not HA-TirNM, recruited N-WASP at the site of intimin-clustered Tir (Fig. 4B). These results suggest that EspH-mediated recruitment of N-WASP is dependent on the C-terminus of Tir independently of Y474.

The WH1 domain of N-WASP is required for EspH-mediated actin polymerization

To investigate the role of N-WASP in EspH-mediated actin polymerization we constructed several deletion variants of murine N-WASP fused to GFP (Fig. 5A), and transfected them into N-WASP-deficient (N-WASP$^{-/-}$) mouse embryonic fibroblasts (MEFs). GFP alone was used as a control. Immunoblotting of N-WASP$^{-/-}$ MEF cell lysates with anti-GFP (Fig. S4A) or anti-N-WASP (Fig. 5B) antibodies showed that the fusion proteins were expressed and stable. We next infected the transfected N-WASP$^{-/-}$ MEFs with E2348/69 expressing Tir$_{WT}$, Tir$_{Y454A/Y474A}$ or coexpressing Tir$_{Y454A/Y474A}$ and EspH-HA. No polymerized actin was detected in GFP transfected MEFs infected with any of the EPEC strains (Fig. 5C and D). Transfection of GFP-N-WASP restored pedestal formation by E2348/69 expressing Tir$_{WT}$, with 91.9 ± 1.3% of microcolonies associated with polymerized actin (Fig. 5C and D). Only 10.8 ± 0.9% of microcolonies were associated with polymerized actin in the GFP-N-WASP transfected cells infected with E2348/69 expressing Tir$_{Y454A/Y474A}$ (Fig. 5C). However, infection of the GFP-N-WASP transfected cells with E2348/69 coexpressing Tir$_{Y454A/Y474A}$ and EspH-HA resulted in 62.7 ± 5.0% of microcolonies associated with polymerized actin and N-WASP recruitment to the site of bacterial adherence (Fig. 5C and D).

We then assessed the importance of the individual domains of N-WASP for EspH-mediated actin polymerization. Deletion of the WASP-homology 1 (GFP-ΔWH1) or proline-rich (GFP-ΔPRD) domains of N-WASP resulted in a marked decrease in pedestal formation by E2348/69 expressing Tir$_{WT}$, as 24.7 ± 7.3% and 56.1 ± 2.1% respectively of EPEC microcolonies were associated with polymerized actin (Fig. 5C). When the transfected MEFs were infected with E2348/69 coexpressing Tir$_{Y454A/Y474A}$ and EspH, only the deletion of the WH1 domain of N-WASP (GFP-ΔWH1) resulted a significant reduction, with 19.8 ± 3.2% of EPEC microcolonies associated with polymerized actin (Fig. 5C and D). Compared with full-length N-WASP, we did not observe a significant difference in actin polymerization triggered by E2348/69 expressing Tir$_{WT}$ or E2348/69 coexpressing Tir$_{Y454A/Y474A}$ and EspH-HA in N-WASP$^{-/-}$ MEFs expressing GFP-N-WASP deletions in Basic (GFP-ΔB), Cdc42/Rac-interactive binding (GFP-ΔCRIB) or GTPase-binding (GFP-ΔGBD) domains (Figs 5C and S4B).

To establish the role of the WH1 domain in EPEC-mediated actin polymerization, we constructed an expression variant with the WH1 domain fused directly to the VCA domain of N-WASP (GFP-WH1-VCA), and ectopically expressed this construct in N-WASP$^{-/-}$ MEFs. Infection with E2348/69 expressing Tir$_{WT}$ resulted in 53.7 ± 4.7% of microcolonies

associated with polymerization actin, compared with 91.9 ± 1.3% of microcolonies associated with polymerization actin in N-WASP$^{-/-}$ MEFs complemented with the full length N-WASP (Fig. 5C and D). However, the GFP-WH1-VCA construct was as functional as the full-length N-WASP in the context of infection with E2348/69 coexpressing $Tir_{Y454A/Y474A}$ and EspH-HA (Fig. 5C and D). Taken together, these results show that both the WH1 and PRD domains are required for efficient Tir-mediated pedestal formation and elongation. Moreover, the WH1 domain of N-WASP is necessary for EspH-mediated actin polymerization.

Disruption of WIP/N-WASP binding abolishes EspH-mediated actin polymerization

The WH1 domain of N-WASP binds the WASP/N-WASP-binding domain (WBD) of WASP interacting protein (WIP) (Volkman *et al.*, 2002). To investigate the role of WIP in triggering EspH-mediated actin polymerization, we transfected Swiss 3T3 fibroblasts with GFP or a GFP-WBD to determine if the latter exhibited a dominant-negative effect. Fluorescence microscopy of GFP-WBD transfected cells infected with E2348/69 expressing Tir_{WT} exhibited a marked reduction in actin polymerization (Fig. 6A), as only 40.1 ± 5.2% of microcolonies formed pedestals (Fig. 6B), which were shorter than those produced in infected control cells (Fig. 6A). Transfection of GFP-WBD severely attenuated EspH-mediated actin polymerization (Fig. 6A), as only 3.4 ± 0.1% of the microcolonies of E2348/69 coexpressing $Tir_{Y454A/Y474A}$ and EspH-HA were associated with polymerized actin (Fig. 6B). These results suggest that WIP is involved in pedestal elongation and that N-WASP recruitment by the EspH pathway is primarily mediated by WIP/N-WASP binding.

EspH and Tir recruit WIP to EPEC attachment sites

The observation that both efficient pedestal formation and EspH-mediated actin polymerization requires WIP/N-WASP suggests that EPEC may utilize two distinct, yet synergistic, actin signalling pathways that converge on WIP recruitment. To test this hypothesis, we constructed an E2348/69Δ*espH* expressing $Tir_{Y454A/Y474A}$ mutant that is deficient in Nck-dependent, NPY-dependent and EspH-mediated actin signalling pathways. We ectopically expressed GFP-WIP in Swiss 3T3 fibroblasts, and infected them with E2348/69 expressing Tir_{WT}, E2348/69Δ*espH* expressing $Tir_{Y454A/Y474A}$, or E2348/69Δ*espH* expressing $Tir_{Y454A/Y474A}$ complemented with either Tir or EspH. GFP-WIP localized to the tip of the pedestal following infection with E2348/69 expressing Tir_{WT} (Fig. 7A). Cells infected with E2348/69Δ*espH* expressing $Tir_{Y454A/Y474A}$ recruited neither WIP nor F-actin. Complementation of the E2348/69Δ*espH* expressing $Tir_{Y454A/Y474A}$ with Tir restored the recruitment of WIP and formation of short actin pedestals (Fig. 7A). Intriguingly, complementation of E2348/69Δ*espH* expressing $Tir_{Y454A/Y474A}$ with EspH induced intense actin rearrangement and formation of a protrusive structure with an actin core surrounded by GFP-WIP. Scanning electron microscopy revealed that these structures are associated with EPEC microcolonies (Fig. 7A). We also transfected N-WASP$^{-/-}$ MEFs with GFP-WIP and infected them with E2348/69 expressing Tir_{WT}, E2348/69Δ*espH* expressing $Tir_{Y454A/Y474A}$ or coexpressing $Tir_{Y454A/Y474A}$ and EspH. None of the strains recruited WIP in the absence of N-WASP (Fig. 7B), suggesting that Tir and EspH recruit WIP in an N-WASP dependent manner. Moreover, these results affirm our hypothesis that the actin signalling pathways mediated by Tir Y474 and EspH converge on WIP and N-WASP.

EspH induces colocalization of WIP, Tir and N-WASP, but not Nck

WIP has been shown to bind to Nck and N-WASP (Anton *et al.*, 1998; Rohatgi *et al.*, 2001; Volkman *et al.*, 2002). To determine if Nck and N-WASP are present at the site of EspH-mediated actin polymerization, Swiss 3T3 fibroblasts transfected with GFP-WIP and infected with E2348/69Δ*espH* expressing $Tir_{Y454A/Y474A}$ complemented with EspH-HA were fixed and stained for Tir, EspH, N-WASP and Nck. Immunofluoresence microscopy revealed that Tir, EspH and N-WASP colocalized with WIP (Fig. 8A).

Interestingly, although WIP can bind Nck *in vitro* (Anton *et al.*, 1998), Nck did not colocalize at the site of bacterial attachment. As a control, we infected the GFP-WIP transfected cells with E348/69 expressing Tir_{WT} and E2348/69Δ*espH* expressing $Tir_{Y454A/Y474A}$. Tir, Nck and N-WASP were all recruited beneath E348/69 expressing Tir_{WT}, but only Tir was recruited beneath E2348/69Δ*espH* expressing $Tir_{Y454A/Y474A}$ (Fig. 8B). These results reaffirm that Nck is not required for EspH-mediated actin polymerization. Taken together, our results show that EspH recruits WIP and N-WASP independently of Nck to trigger localized actin polymerization and promote elongation of Nck-mediated actin pedestals (Fig. 9).

Discussion

In this paper we report that EspH promotes N-WASP recruitment and Arp2/3-mediated actin polymerization independently of Tir residues Y454 and Y474 and by extension the Tir:Nck and Tir:IRTKS/IRSp53 actin signalling pathways. Accordingly, EPEC triggers localized actin polymerization by parallel mechanisms that eventually converge on WIP and N-WASP, and that WIP is required for efficient formation and elongation of EPEC actin pedestals.

Using deletion variants of N-WASP, we identified WH1 and PRD domains as important regions for Tir-mediated actin pedestal formation. Consistent with this observation, the expression of a WBD construct exerted a dominant-negative effect that markedly reduced pedestal formation and elongation. This observation differs from a previous report that the PRD domain of N-WASP is dispensable for actin pedestal formation, and that the WBD construct did not exert a dominant-negative effect on actin pedestal formation (Lommel *et al.*, 2001). Furthermore, it was previously reported that WIP is found throughout the pedestal length (Lommel *et al.*, 2001), while we observed that WIP mainly localizes to the tip of pedestals together with Tir, Nck and N-WASP, suggesting that WIP might have an active role at the site of actin nucleation. As N-WASP is required for WIP recruitment to the bacterial attachment site, both proteins appear to be recruited in complex. Since WIP can also binds Nck (Anton *et al.*, 1998; Rohatgi *et al.*, 2001), our results give further evidence for a model whereby the Tir:Nck pathway recruits a WIP/N-WASP complex via both Nck/WIP and Nck/N-WASP interactions that synergistically trigger actin polymerization in a process similar to *Vaccinia* virus actin-based motility (Moreau *et al.*, 2000).

Intriguingly, EspH is also able to promote the recruitment of WIP and N-WASP independently of Nck or repression of Rho GTPases. Moreover, while the CRIB domain of N-WASP, which binds activated Rho GTPases, was dispensable, dominant-negative WIP abolished EspH-mediated actin polymerization. Expression of GFP-WIP during infection

with E2348/69 coexpressing $Tir_{Y454A/Y474A}$ and EspH induced extensive actin cytoskeletal rearrangements at the site of bacterial attachment. This unique actin structure is characterized by the recruitment of Tir, EspH, WIP and N-WASP, but not Nck, around an actin core. Our results suggest that EspH promotes Nck-independent WIP and N-WASP recruitment via an unknown pathway and enhances Nck-mediated actin pedestal formation and elongation. Indeed, WIP overexpression has previously been reported to increase F-actin content and induce formation of subcortical actin clusters in human B cell lines (Ramesh *et al.*, 1997).

A question that remains unanswered is why endogenous levels of EspH are insufficient to trigger localized actin polymerization during EPEC infection. This question is not limited to EspH as phenotypes of other cytoskeletal-modulating T3SS effectors, e.g. EspV (Arbeloa *et al.*, 2011), EspT (Bulgin *et al.*, 2009) and EspM (Arbeloa *et al.*, 2008), could only be seen using *in vitro* cell models following overexpression. This might reflect the existence of a complex regulatory mechanism of effectors expression and translocation *in vivo*, which we do not yet understand, that the cell culture conditions do not mimic. Alternatively, overexpression of EspH may simply shorten the length of time needed by EPEC to initiate EspH-mediated actin polymerization, which endogenous levels could only achieve beyond the viability of the infected monolayer. Nevertheless, EspH has previously been shown to be important for bacterial adherence and colonization *in vivo* (Ritchie and Waldor, 2005; Shaw *et al.*, 2005). Coupled with the observation that Tir:Nck and Tir:IRTKS/IRSp53 pathways play a role in the *in vivo* competitiveness of *C. rodentium* in mice and EHEC in rabbits (Ritchie and Waldor, 2005; Crepin *et al.*, 2009), our data suggest that just as $TccP/EspF_U$ in EHEC (Garmendia *et al.*, 2004; 2006; Campellone *et al.*, 2004b; Cheng *et al.*, 2008; Sallee *et al.*, 2008) and EPEC lineage 2 (Whale *et al.*, 2006) strains is able to amplify the inefficient Tir:IRTKS/IRSp53 actin polymerization pathway, EspH might contribute to competitiveness and *in vivo* fitness of A/E pathogens by intensifying actin polymerization pathways through WIP, in a mechanism dependent on the C-terminus of Tir.

The mechanism by which EspH recruits WIP to the bacterial attachment site remains elusive. As we were unable to co-immunoprecipitate EspH with WIP or N-WASP (data not shown), it is unlikely that EspH directly binds WIP/N-WASP to drive actin polymerization. Since Nck is not recruited during EspH-mediated actin polymerization, other adaptor protein/s are likely to be involved in the EspH-mediated actin signalling upstream of WIP. Indeed, EspH localizes to the plasma membrane and promiscuously binds DH-PH containing RhoGEFs (Dong *et al.*, 2010), which contain other domains such as regulator of G-protein signalling (RGS) and Src-homology 3 (SH3) domains (Rossman *et al.*, 2005). It is thus possible that EspH could recruit WIP/N-WASP complex via interactions with specific RhoGEFs. For example, intersectin is a Cdc42-specific GEF that is able to bind directly to N-WASP via its SH3 domain to promote actin polymerization in a positive feedback loop (Hussain *et al.*, 2001). Interestingly, previous studies also demonstrate that the WIP/N-WASP complex can localize and trigger actin polymerization dependent on the curvature of the membrane (Takano *et al.*, 2008). EspH could thus trigger actin polymerization at the plasma membrane as an indirect result of its ability to induce dramatic changes to cell shape (Tu *et al.*, 2003; Dong *et al.*, 2010). Further work is required to determine if membrane dynamics play a role in modulating EspH-mediated actin remodelling.

In assessing the role of EspH during EPEC infection, we found that like many EPEC T3SS effectors, e.g. NleH effectors that can subvert NF-κB function (Gao *et al.*, 2009) and block apoptosis (Hemrajani *et al.*, 2010), EspH is multi-functional. EspH blocks the activation of Rho GTPases by inactivating endogenous mammalian RhoGEFs to inhibit phagocytosis (Dong *et al.*, 2010), but also plays an additional role in recruiting WIP to the site of bacterial adherence to promote actin polymerization and pedestal elongation. Our results also demonstrate the intricate complexities of Tir and EspH-mediated actin polymerization that involves distinct, convergent and synergistic signalling cascades.

Experimental procedures

Bacterial strains and plasmids

Bacterial strains and plasmids used in this study are listed in Tables 1 and 2. Bacteria were grown from single colonies in Luria–Bertani (LB) broth in a shaking incubator at 37°C, except those transformed with the temperature-sensitive pKD46 plasmid (30°C). Culture media or agar was supplemented with ampicillin (100 μg ml^{-1}), chloramphenicol (34 μg ml^{-1}) or kanamycin (50 μg ml^{-1}) as appropriate. Bacterial cultures were primed for infection by dilution of 1:100 of overnight bacterial culture with pre-warmed in Dulbecco's minimal Eagle media (DMEM) high glucose (4500 mg l^{-1}) (Sigma), and incubated as static cultures at 37°C in 5% CO_2 for 3 h. Static cultures were induced with 1 mM Isopropyl thio-galactopyranoside for pSA10-effector expression 30 min prior to infection.

EPEC tir *mutagenesis*

E2348/69 strains expressing mutated Tir were generated using a lambda red-based mutagenesis system (Datsenko and Wanner, 2000; Crepin *et al.*, 2009), via the introduction of site-directed *tir* mutagenesis into the endogenous chromosomal *tir* gene together with a kanamycin cassette in the *tir-cesT* intergenic region as previously described. Primers are listed in Table 3. To mutate the C-terminus tyrosine residues of *tir*, the 3′ end of *tir*, followed by a non-polar *aphT* cassette, and then the *tir-cesT* intergenic region and 5′ end of *cesT* were first cloned into pGEMT vector. The 3′ end of *tir* was amplified using primer pair TirC-E69-Fw/EcoRI-TirC-E69-Rv, while the intergenic region and 5′ end of *cesT* was amplified using primer pair EcoRI-NcesT-E69-Fw/NcesT-E69-Rv. Both fragments were then digested with EcoRI, ligated together, and then cloned into pGEMT. The non-polar *aphT* cassette was then inserted into the EcoRI site between the two fragments and the orientation of the *aphT* cassette ascertained by PCR. This plasmid, pICC530, was used to generate the control mutant Tir_{WT}.

EPEC *tir* mutagenesis was carried out by inverse-PCR using pICC530. The primer pairs TirC-E69-Y454A-Fw/TirC-E69-Y454A-Rv and TirC-E69-Y474A-Fw/TirC-E69-Y474A-Rv were used to mutate the tyrosine residues Y454 and Y474 into alanines (Tir_{Y454A} and Tir_{Y474A}) generating pICC531 and pICC532 respectively. The double tyrosine mutant ($Tir_{Y454A/Y474A}$) was generated by superimposing Y474A on the Y454A mutant, generating pICC533. All pGEMT derivatives were checked by DNA sequencing. To introduce tir_{WT}, tir_{Y454A}, tir_{Y474A} and $tir_{Y454A/Y474A}$ site-directed mutants into bacterial chromosome, the inserts in all pGEMT derivatives were amplified using the primer pair TirC-E69-Fw/NcesT-

E69-Rv. The PCR products were electroporated into E2348/69 containing pKD46 encoding lambda red recombinase. Transformants were selected on kanamycin agar plates and the insertion of site-directed *tir* mutants confirmed by PCR and DNA sequencing.

E2348/69ΔespH $Tir_{Y454A/Y474A}$ mutagenesis

A 325 bp upstream region of *espH* was amplified using primer pair Up-EspH-E69-Fw/BamHI-Up-EspH-E69-Rv, and a 499 bp downstream region of *espH* was amplified using primer pair BamHI-Dn-EspH-E69-Fw/Dn-EspH-E69-Rv. Both fragments were then digested with BamHI, ligated together, and then cloned into pGEMT The non-polar *cat* cassette was then inserted into the BamHI site between the two fragments and the orientation of the *cat* cassette ascertained by PCR. This plasmid, pICC628, was then amplified using the primer pair Up-EspH-E69-Fw/Dn-EspH-E69-Rv. The PCR products were electroporated into E23478/69 $Tir_{Y454A/Y474A}$ containing pKD46 encoding lambda red recombinase. Transformants were selected on chloramphenicol agar plates and *espH* deletion confirmed by PCR and DNA sequencing.

Construction of GFP-N-WASP and HA-TirNM expression variants

Construction of the different GFP-NWASP expression variants was carried out by inverse PCR, using pEGFP-N-WASP expression vector (kindly provided by Dr. Emmanuelle Caron) as template. The primer pairs NWASP-WH1del-Rv/NWASP-WH1del-Fw, NWASP-Bdel-Rv/NWASP-Bdel-Fw, NWASP-CRIBdel-Rv/NWASP-CRIBdel-Fw, NWASP-CRIBdel-Rv/NWASP-GBDdel-Fw, NWASP-PRDdel-Rv/NWASP-PRDdel-Fw and NWASP-WH1del-Rv/NWASP-PRDdel-Fw were used to delete the WH1 (1–156), B (156–200), CRIB (200–226), GBD (226–274), PRD (274–392) and all domains except WH1 (156–392), generating GFP-ΔWH1, GFP-ΔB, GFP-ΔCRIB, GFP-ΔGBD, GFP-ΔPRD and GFP-WH1-VCA respectively. All pEGFP-N-WASP expression variants were sequenced and assessed with Western blot analysis to ensure stable expression.

Construction of HA-TirNM was carried out first by re-inserting the N-terminus of Tir (aa 1–233) into the HindIII restriction site of pCDNA3-TirMC to generate pICC626. Using pICC626 as template, the primer pairs pCDNA3-TirNM(EPEC)-Rv/pCDNA3-TirNM(EPEC)-Fw was used to delete the C-terminus of Tir (aa 388–547), generating pCDN3-TirNM. All pCDNA3-Tir expression variants were sequenced and assessed for membrane localization by transfection.

siRNA knockdown of Rho GTPases

For siRNA knockdown of Cdc42, Rac1 and RhoA, siRNA pool sequences were selected from a proprietary Rho GTPase siRNA library (Dharmacon). siRNA knockdown was performed on Swiss 3T3 fibroblasts using HiPerfect (Qiagen) according to manufacturer's instructions. siRNA knockdown was allowed to proceed at 37°C in a humidified incubator with 5% CO_2 for 48 h before EPEC infection. Effectiveness of RNAi-mediated gene silencing of Rho GTPases was assessed by Western blot using the appropriate antibodies.

Transfection and Infection of cells with EPEC E2348/69

Swiss 3T3 fibroblasts (ATCC CCL-92), $Nck^{-/-}$ fibroblasts (Bladt *et al.*, 2003) and N-$WASP^{-/-}$ mouse embryonic fibroblasts (MEFs) were grown at 37°C in a humidified atmosphere containing 5% CO_2 in DMEM high glucose (4500 mg l^{-1}) (Sigma) supplemented with 10% (v/v) heat-inactivated fetal bovine serum (Gibco) and 2 mM glutamax (Sigma). Cells were grown in 24-well cell culture plates to 80% confluence. Cells were transfected in serum-free DMEM with mammalian expression vectors using lipofectamine2000 (Invitrogen) according to the manufacturer's instructions. Transfected cells were incubated at 37°C in a humidified incubator with 5% CO_2 for 4 h before having their media replaced with pre-warmed serum-containing DMEM, and incubated for a further 20 h unless otherwise stated. Monolayers were washed twice with PBS and then infected with 0.5 ml of primed bacterial culture at 37°C in a humidified atmosphere containing 5% CO_2 for 2 h unless otherwise stated. Coverslips were washed three times in PBS and fixed with 3% paraformaldehyde for 15 min before being processed for immunofluorescence microscopy.

Immunofluorescence microscopy

Cells were quenched for 15 min with 50 mM NH_4Cl, and then permeabilized for 5 min in PBS/0.2% Triton X-100. Coverslips were washed thrice in PBS and blocked in PBS/1% BSA for 10 min before addition of primary antibodies. Coverslips were incubated with primary antibodies diluted in PBS/1% BSA for 1 h. After washing thrice with PBS, coverslips were then incubated with secondary antibodies diluted in PBS/1% BSA for a further 1 h. Coverslips were washed thrice again PBS and once in water before being mounted in Gold Pro-Long Anti-fade medium (Invitrogen), and examined by conventional epifluoresecence microscopy using a Zeiss Axio LSM-510 microscope. Images were deconvoluted and processed using Zeiss Axiovision 4.8 software and Adobe Photoshop CS4.

Antibodies

Actin was detected with Oregon Green conjugated Phalloidin antibody (1:100 dilution) (Invitrogen) or TRITC-conjugated Phalloidin (1:500 dilution) (Sigma). Intimin or Tir were labelled with polyclonal chicken anti-intimin (1:200 dilution) or anti-Tir (1:500 dilution) antibody serum respectively (kindly provided by Dr Roberto La Ragione, Veterinary Laboratory Agency, UK). Arp2/3 complex was visualized using mouse anti-Arp2 subunit antibody (1:200 dilution) (kindly provided by Laura Machesky). N-WASP was visualized using a polyclonal rabbit anti-N-WASP antibody (1:100 dilution) (Sigma). Nck was visualized using a polyclonal rabbit anti-Nck antibody (1:100 dilution) (Millipore/Upstate). HA-tagged proteins were labelled with monoclonal anti-HA.11 (1:500 dilution) (Covance), while transfected cells expressing myc-tagged proteins were labelled with monoclonal anti-myc antibody (1:500 dilution) (Millipore). Cy2, RRX or Cy5 conjugated donkey anti-mouse, anti-chicken or anti-rabbit antibodies (1:200 dilution) (Jackson ImmunoResearch) were used as secondary antibodies.

Europe PMC Funders Author Manuscripts

Scanning electron microscopy

Cells were infected as previously described, and fixed in 2.5% glutaraldehyde PBS overnight at 4°C. Coverslips were then washed thrice in PBS for 1.5 h with regular changes. Cells were further post-fixed in aqueous 1% osmium tetroxide (OsO_4), rinsed in water, then dehydrated in a graded series of 50%, 75%, 85%, 95% and 100% ethanol. Samples were processed for scanning electron microscopy using an Emitech K850 critical-point drier, coated with gold–palladium for 90 s using a Polaron SC7620 mini sputter-coater, and examined using a JEOL JSM-6390 scanning electron microscope.

Western blot

Proteins were extracted from cells using RIPA buffer. Samples were separated on a 12% polyacrylamide gel, and transferred to nitrocellulose membrane (Bio-Rad). Blots were then blocked in TBS/0.1% Tween-20 containing 5% BSA and probed with polyclonal rabbit anti-Cdc42 (BD Biosciences), monoclonal mouse anti-Rac1 (Cell Signalling), polyclonal rabbit anti-RhoA (Santa Cruz), polyclonal rabbit anti-N-WASP (Sigma) (1:1000 dilution) or anti-GFP (Abcam) (1:1000 dilution) overnight at 4°C. After washing, immunoreactive bands were visualized using horseradish peroxidase-linked secondary antibodies (1:10 000 dilution) (Jackson ImmunoResearch) and ECL reagent (GE Healthcare). Chemiluminescence was detected using a LAS-3000 Fuji Imager.

Statistical analysis

Results were expressed as mean ± standard deviation. Statistical significance was determined by an unpaired two-tailed *t*-test. A *P*-value of < 0.01 was considered to be significant.

Supporting information

Refer to Web version on PubMed Central for supplementary material.

Acknowledgements

We thank Dr Roberto La Ragione (Veterinary Laboratory Agency, UK) for the anti-O127 antibodies, Dr Laura Machesky (Beatson Institute, Glasgow) for the anti-Arp2 antibody and pRK5myc-IRSp53 and pRK5myc-WAVE2 expression vectors, Dr Scott Snapper (Harvard Medical School, Boston) for the N-WASP knockout cell line, Dr Michael Way (Cancer Research, UK) for the GFP-WIP and GFP-WBD expression vectors, and the late Dr Emmanuelle Caron for the pEGFP-N-WASP expression vector. This work was supported by grants from the Wellcome Trust.

References

Anton IM, Lu W, Mayer BJ, Ramesh N, Geha RS. The Wiskott–Aldrich syndrome protein-interacting protein (WIP) binds to the adaptor protein Nck. J Biol Chem. 1998; 273:20992–20995. [PubMed: 9694849]

Arbeloa A, Bulgin RR, MacKenzie G, Shaw RK, Pallen MJ, Crepin VF, et al. Subversion of actin dynamics by EspM effectors of attaching and effacing bacterial pathogens. Cell Microbiol. 2008; 10:1429–1441. [PubMed: 18331467]

Arbeloa A, Oates CV, Marches O, Hartland EL, Frankel G. Enteropathogenic and enterohemorrhagic *Escherichia coli* type III secretion effector EspV induces radical morphological changes in eukaryotic cells. Infect Immun. 2011; 79:1067–1076. [PubMed: 21189318]

Europe PMC Funders Author Manuscripts

Aspenstrom P. The WASP-binding protein WIRE has a role in the regulation of the actin filament system downstream of the platelet-derived growth factor receptor. Exp Cell Res. 2002; 279:21–33. [PubMed: 12213210]

Berger CN, Crepin VF, Jepson MA, Arbeloa A, Frankel G. The mechanisms used by enteropathogenic *Escherichia coli* to control filopodia dynamics. Cell Microbiol. 2009; 11:309–322. [PubMed: 19046338]

Bladt F, Aippersbach E, Gelkop S, Strasser GA, Nash P, Tafuri A, et al. The murine Nck SH2/SH3 adaptors are important for the development of mesoderm-derived embryonic structures and for regulating the cellular actin network. Mol Cell Biol. 2003; 23:4586–4597. [PubMed: 12808099]

Bommarius B, Maxwell D, Swimm A, Leung S, Corbett A, Bornmann W, Kalman D. Enteropathogenic *Escherichia coli* Tir is an SH2/3 ligand that recruits and activates tyrosine kinases required for pedestal formation. Mol Microbiol. 2007; 63:1748–1768. [PubMed: 17367393]

Brady MJ, Campellone KG, Ghildiyal M, Leong JM. Enterohaemorrhagic and enteropathogenic *Escherichia coli* Tir proteins trigger a common Nck-independent actin assembly pathway. Cell Microbiol. 2007; 9:2242–2253. [PubMed: 17521329]

Bulgin RR, Arbeloa A, Chung JC, Frankel G. EspT triggers formation of lamellipodia and membrane ruffles through activation of Rac-1 and Cdc42. Cell Microbiol. 2009; 11:217–229. [PubMed: 19016787]

Campellone KG, Leong JM. Nck-independent actin assembly is mediated by two phosphorylated tyrosines within enteropathogenic *Escherichia coli* Tir. Mol Microbiol. 2005; 56:416–432. [PubMed: 15813734]

Campellone KG, Rankin S, Pawson T, Kirschner MW, Tipper DJ, Leong JM. Clustering of Nck by a 12-residue Tir phosphopeptide is sufficient to trigger localized actin assembly. J Cell Biol. 2004a; 164:407–416. [PubMed: 14757753]

Campellone KG, Robbins D, Leong JM. EspFU is a translocated EHEC effector that interacts with Tir and N-WASP and promotes Nck-independent actin assembly. Dev Cell. 2004b; 7:217–228. [PubMed: 15296718]

Cheng HC, Skehan BM, Campellone KG, Leong JM, Rosen MK. Structural mechanism of WASP activation by the enterohaemorrhagic *E. coli* effector EspF(U). Nature. 2008; 454:1009–1013. [PubMed: 18650809]

Crepin VF, Girard F, Schuller S, Phillips AD, Mousnier A, Frankel G. Dissecting the role of the Tir:Nck and Tir:IRTKS/IRSp53 signalling pathways *in vivo*. Mol Microbiol. 2009; 75:308–323. [PubMed: 19889090]

Datsenko KA, Wanner BL. One-step inactivation of chromosomal genes in *Escherichia coli* K-12 using PCR products. Proc Natl Acad Sci USA. 2000; 97:6640–6645. [PubMed: 10829079]

Dong N, Liu L, Shao F. A bacterial effector targets host DH-PH domain RhoGEFs and antagonizes macrophage phagocytosis. EMBO J. 2010; 29:1363–1376. [PubMed: 20300064]

Frankel G, Phillips AD. Attaching effacing *Escherichia coli* and paradigms of Tir-triggered actin polymerization: getting off the pedestal. Cell Microbiol. 2008; 10:549–556. [PubMed: 18053003]

Galan JE, Ginocchio C, Costeas P. Molecular and functional characterization of the *Salmonella* invasion gene invA: homology of InvA to members of a new protein family. J Bacteriol. 1992; 174:4338–4349. [PubMed: 1624429]

Gao X, Wan F, Mateo K, Callegari E, Wang D, Deng W, et al. Bacterial effector binding to ribosomal protein s3 subverts NF-kappaB function. PLoS Pathog. 2009; 5:e1000708. [PubMed: 20041225]

Garmendia J, Phillips AD, Carlier MF, Chong Y, Schuller S, Marches O, et al. TccP is an enterohaemorrhagic *Escherichia coli* O157:H7 type III effector protein that couples Tir to the actin-cytoskeleton. Cell Microbiol. 2004; 6:1167–1183. [PubMed: 15527496]

Garmendia J, Carlier MF, Egile C, Didry D, Frankel G. Characterization of TccP-mediated N-WASP activation during enterohaemorrhagic *Escherichia coli* infection. Cell Microbiol. 2006; 8:1444–1455. [PubMed: 16922863]

Gruenheid S, DeVinney R, Bladt F, Goosney D, Gelkop S, Gish GD, et al. Enteropathogenic *E. coli* Tir binds Nck to initiate actin pedestal formation in host cells. Nat Cell Biol. 2001; 3:856–859. [PubMed: 11533668]

Hartland EL, Batchelor M, Delahay RM, Hale C, Matthews S, Dougan G, et al. Binding of intimin from enteropathogenic *Escherichia coli* to Tir and to host cells. Mol Microbiol. 1999; 32:151–158. [PubMed: 10216868]

Hemrajani C, Berger CN, Robinson KS, Marches O, Mousnier A, Frankel G. NIeH effectors interact with Bax inhibitor-1 to block apoptosis during enteropathogenic *Escherichia coli* infection. Proc Natl Acad Sci USA. 2010; 107:3129–3134. [PubMed: 20133763]

Ho HY, Rohatgi R, Ma L, Kirschner MW. CR16 forms a complex with N-WASP in brain and is a novel member of a conserved proline-rich actin-binding protein family. Proc Natl Acad Sci USA. 2001; 98:11306–11311. [PubMed: 11553796]

Hussain NK, Jenna S, Glogauer M, Quinn CC, Wasiak S, Guipponi M, et al. Endocytic protein intersectin-l regulates actin assembly via Cdc42 and N-WASP. Nat Cell Biol. 2001; 3:927–932. [PubMed: 11584276]

Jerse AE, Kaper JB. The *eae* gene of enteropathogenic *Escherichia coli* encodes a 94-kilodalton membrane protein, the expression of which is influenced by EAF plasmid. Infect Immun. 1991; 59:4302–4309. [PubMed: 1682258]

Kato M, Miki H, Kurita S, Endo T, Nakagawa H, Miyamoto S, Takenawa T. WICH, a novel verprolin homology domain-containing protein that functions cooperatively with N-WASP in actin-microspike formation. Biochem Biophys Res Commun. 2002; 291:41–47. [PubMed: 11829459]

Kenny B. Phosphorylation of tyrosine 474 of the enteropathogenic *Escherichia coli* (EPEC) Tir receptor molecule is essential for actin nucleating activity and is preceded by additional host modifications. Mol Microbiol. 1999; 31:1229–1241. [PubMed: 10096089]

Kenny B, DeVinney R, Stein M, Reinscheid DJ, Frey EA, Finlay BB. Enteropathogenic *E. coli* (EPEC) transfers its receptor for intimate adherence into mammalian cells. Cell. 1997; 91:511–520. [PubMed: 9390560]

Knutton S, Lloyd DR, McNeish AS. Adhesion of enteropathogenic *Escherichia coli* to human intestinal enterocytes and cultured human intestinal mucosa. Infect Immun. 1987; 55:69–77. [PubMed: 3539808]

Levine MM, Berquist EJ, Nalin DR, Waterman DH, Hornick RB, Young CR, Sotman S. *Escherichia coli* strains that cause diarrhoea but do not produce heat-labile or heat-stable enterotoxins and are non-invasive. Lancet. 1978; 1:1119–1122. [PubMed: 77415]

Lommel S, Benesch S, Rottner K, Franz T, Wehland J, Kuhn R. Actin pedestal formation by enteropathogenic *Escherichia coli* and intracellular motility of *Shigella flexneri* are abolished in N-WASP-defective cells. EMBO Rep. 2001; 2:850–857. [PubMed: 11559594]

Millard TH, Dawson J, Machesky LM. Characterisation of IRTKS, a novel IRSp53/MIM family actin regulator with distinct filament bundling properties. J Cell Sci. 2007; 120:1663–1672. [PubMed: 17430976]

Moreau V, Frischknecht F, Reckmann I, Vincentelli R, Rabut G, Stewart D, Way M. A complex of N-WASP and WIP integrates signalling cascades that lead to actin polymerization. Nat Cell Biol. 2000; 2:441–448. [PubMed: 10878810]

Mundy R, MacDonald TT, Dougan G, Frankel G, Wiles S. *Citrobacter rodentium* of mice and man. Cell Microbiol. 2005; 7:1697–1706. [PubMed: 16309456]

Nataro JP, Kaper JB. Diarrheagenic *Escherichia coli*. Clin Microbiol Rev. 1998; 11:142–201. [PubMed: 9457432]

Padrick SB, Rosen MK. Physical mechanisms of signal integration by WASP family proteins. Ann Rev Biochem. 2010; 79:707–735. [PubMed: 20533885]

Peterson FC, Deng Q, Zettl M, Prehoda KE, Lim WA, Way M, Volkman BF. Multiple WASPinteracting protein recognition motifs are required for a functional interaction with N-WASP. J Biol Chem. 2007; 282:8446–8453. [PubMed: 17229736]

Phillips N, Hayward RD, Koronakis V. Phosphorylation of the enteropathogenic *E. coli* receptor by the Src-family kinase c-Fyn triggers actin pedestal formation. Nat Cell Biol. 2004; 6:618–625. [PubMed: 15220932]

Ramesh N, Anton IM, Hartwig JH, Geha RS. WIP, a protein associated with Wiskott–Aldrich syndrome protein, induces actin polymerization and redistribution in lymphoid cells. Proc Natl Acad Sci USA. 1997; 94:14671–14676. [PubMed: 9405671]

Ritchie JM, Waldor MK. The locus of enterocyte effacement-encoded effector proteins all promote enterohemorrhagic *Escherichia coli* pathogenicity in infant rabbits. Infect Immun. 2005; 73:1466–1474. [PubMed: 15731044]

Rohatgi R, Ma L, Miki H, Lopez M, Kirchhausen T, Takenawa T, Kirschner MW. The interaction between N-WASP and the Arp2/3 complex links Cdc42-dependent signals to actin assembly. Cell. 1999; 97:221–231. [PubMed: 10219243]

Rohatgi R, Nollau P, Ho HY, Kirschner MW, Mayer BJ. Nck and phosphatidylinositol 4,5-bisphosphate synergistically activate actin polymerization through the N-WASP-Arp2/3 pathway. J Biol Chem. 2001; 276:26448–26452. [PubMed: 11340081]

Rossman KL, Der CJ, Sondek J. GEF means go: turning on RHO GTPases with guanine nucleotide-exchange factors. Nat Rev Mol Cell Biol. 2005; 6:167–180. [PubMed: 15688002]

Sallee NA, Rivera GM, Dueber JE, Vasilescu D, Mullins RD, Mayer BJ, Lim WA. The pathogen protein EspF(U) hijacks actin polymerization using mimicry and multivalency. Nature. 2008; 454:1005–1008. [PubMed: 18650806]

Shaw RK, Cleary J, Murphy MS, Frankel G, Knutton S. Interaction of enteropathogenic *Escherichia coli* with human intestinal mucosa: role of effector proteins in brush border remodeling and formation of attaching and effacing lesions. Infect Immun. 2005; 73:1243–1251. [PubMed: 15664974]

Swimm A, Bommarius B, Li Y, Cheng D, Reeves P, Sherman M, et al. Enteropathogenic *Escherichia coli* use redundant tyrosine kinases to form actin pedestals. Mol Biol Cell. 2004; 15:3520–3529. [PubMed: 15155808]

Takano K, Toyooka K, Suetsugu S. EFC/F-BAR proteins and the N-WASP-WIP complex induce membrane curvature-dependent actin polymerization. EMBO J. 2008; 27:2817–2828. [PubMed: 18923421]

Takenawa T, Suetsugu S. The WASP-WAVE protein network: connecting the membrane to the cytoskeleton. Nat Rev Mol Cell Biol. 2007; 8:37–48. [PubMed: 17183359]

Tu X, Nisan I, Yona C, Hanski E, Rosenshine I. EspH, a new cytoskeleton-modulating effector of enterohaemorrhagic and enteropathogenic *Escherichia coli*. Mol Microbiol. 2003; 47:595–606. [PubMed: 12535063]

Vingadassalom D, Kazlauskas A, Skehan B, Cheng HC, Magoun L, Robbins D, et al. Insulin receptor tyrosine kinase substrate links the *E. coli* O157:H7 actin assembly effectors Tir and EspF(U) during pedestal formation. Proc Natl Acad Sci USA. 2009; 106:6754–6759. [PubMed: 19366662]

Volkman BF, Prehoda KE, Scott JA, Peterson FC, Lim WA. Structure of the N-WASP EVH1 domain-WIP complex: insight into the molecular basis of Wiskott–Aldrich syndrome. Cell. 2002; 111:565–576. [PubMed: 12437929]

Weiler MC, Smith JL, Masters JN. CR16, a novel proline-rich protein expressed in rat brain neurons, binds to SH3 domains and is a MAP kinase substrate. J Mol Neurosci. 1996; 7:203–215. [PubMed: 8906616]

Weiss SM, Ladwein M, Schmidt D, Ehinger J, Lommel S, Stading K, et al. IRSp53 links the enterohemorrhagic *E. coli* effectors Tir and EspFU for actin pedestal formation. Cell Host Microbe. 2009; 5:244–258. [PubMed: 19286134]

Whale AD, Garmendia J, Gomes TA, Frankel G. A novel category of enteropathogenic *Escherichia coli* simultaneously utilizes the Nck and TccP pathways to induce actin remodelling. Cell Microbiol. 2006; 8:999–1008. [PubMed: 16681840]

Wong AR, Pearson JS, Bright MD, Munera D, Robinson KS, Lee SF, et al. Enteropathogenic and enterohaemorrhagic *Escherichia coli:* even more subversive elements. Mol Microbiol. 2011; 80:1420–1438. [PubMed: 21488979]

Europe PMC Funders Author Manuscripts

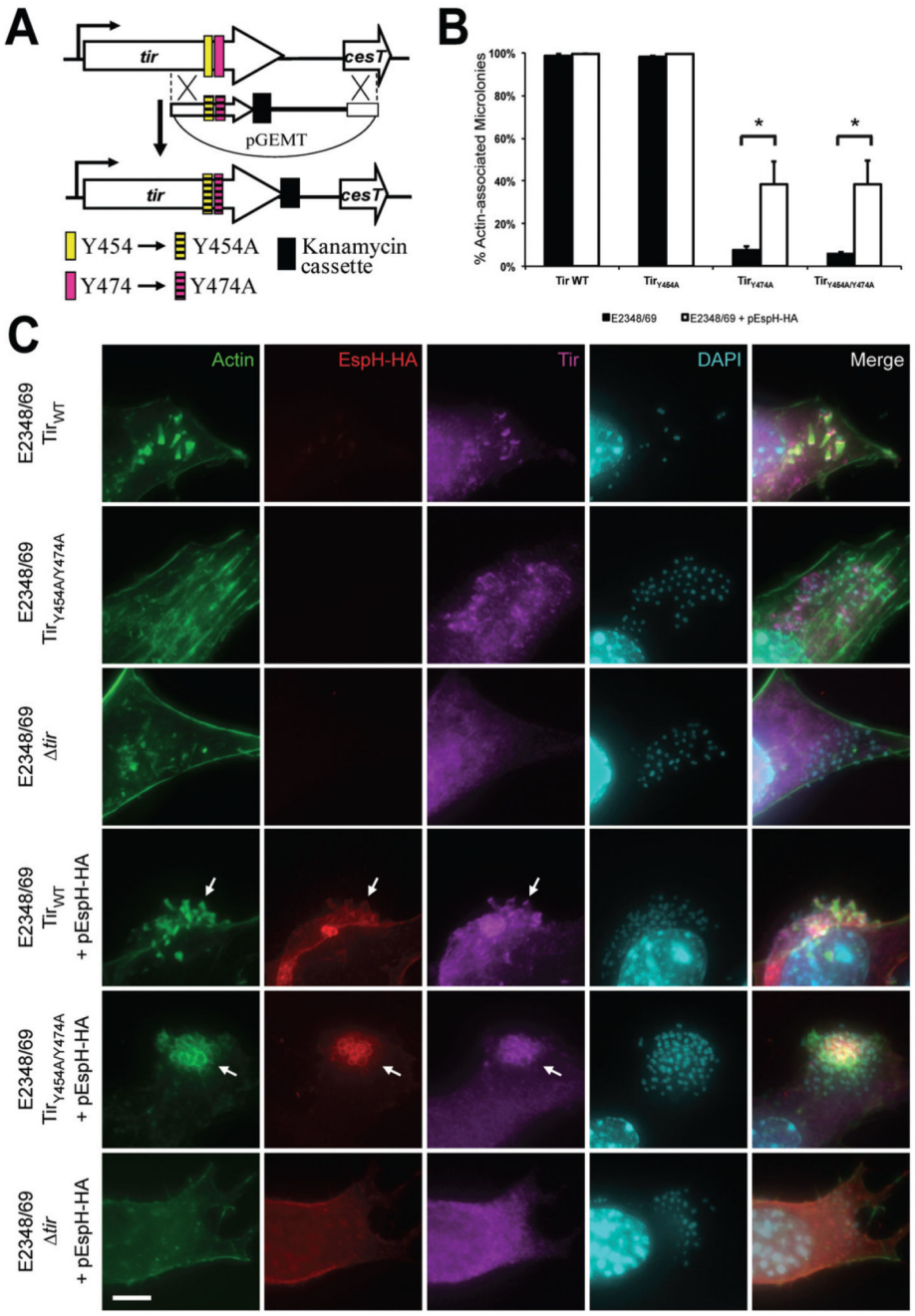

Fig. 1. EspH localizes to plasma membrane surrounding actin pedestals and promotes localized actin polymerization independently of Tir tyrosine residues Y454 and Y474.

A. Schematic representation of tir_{EPEC} chromosomal mutagenesis strategy. Amplified fragments of recombinant pGEMT plasmids containing *tir* Y454 and/or Y474 mutations were used to introduce the mutations in tandem with an *aphT* kanamycin-resistance cassette into the endogenous tir_{EPEC} locus to generate E2348/69 Tir_{Y454A}, Tir_{Y474A} and $Tir_{Y454A/Y474A}$ mutants. As a control recombination of *tir*, an *aphT* kanamycin-resistance cassette with no mutations was inserted (E2348/69 Tir_{WT}).

B. Quantification of EPEC microcolonies associated with actin on cells infected with E2348/69 expressing Tir_{WT}, Tir_{Y454A}, Tir_{Y474A} or $Tir_{Y454A/Y474A}$, with or without EspH-HA (pEspH-HA). A total of 100 microcolonies were counted in triplicates. Results are presented as a mean ± SD of three independent experiments. Asterisks indicate statistical significance ($P < 0.01$).

C. Infection of Swiss 3T3 fibroblasts with E2348/69 expressing Tir_{WT}, $Tir_{Y454A/Y474A}$ or E2348/69Δ*tir*, with or without plasmid-expressed haemagglutinin-tagged EspH (pEspH-HA). Actin was stained with Oregon green phalloidin (green), HA-tagged EspH was detected with anti-HA antibody (red), Tir was detected with anti-Tir antibody (magenta) and bacteria were visualized with DAPI staining (cyan). EspH localized to the pedestal membrane (arrows). Ectopic expression of EspH induced localized F-actin accumulation under E2348/69 expressing $Tir_{Y454A/Y474A}$ (arrows), but not E2348/69 $Tir_{Y454A/Y474A}$ alone. No detection of actin was observed in E2348/69Δ*tir* + pEspH. Bar = 5 μm.

Europe PMC Funders Author Manuscripts

Europe PMC Funders Author Manuscripts

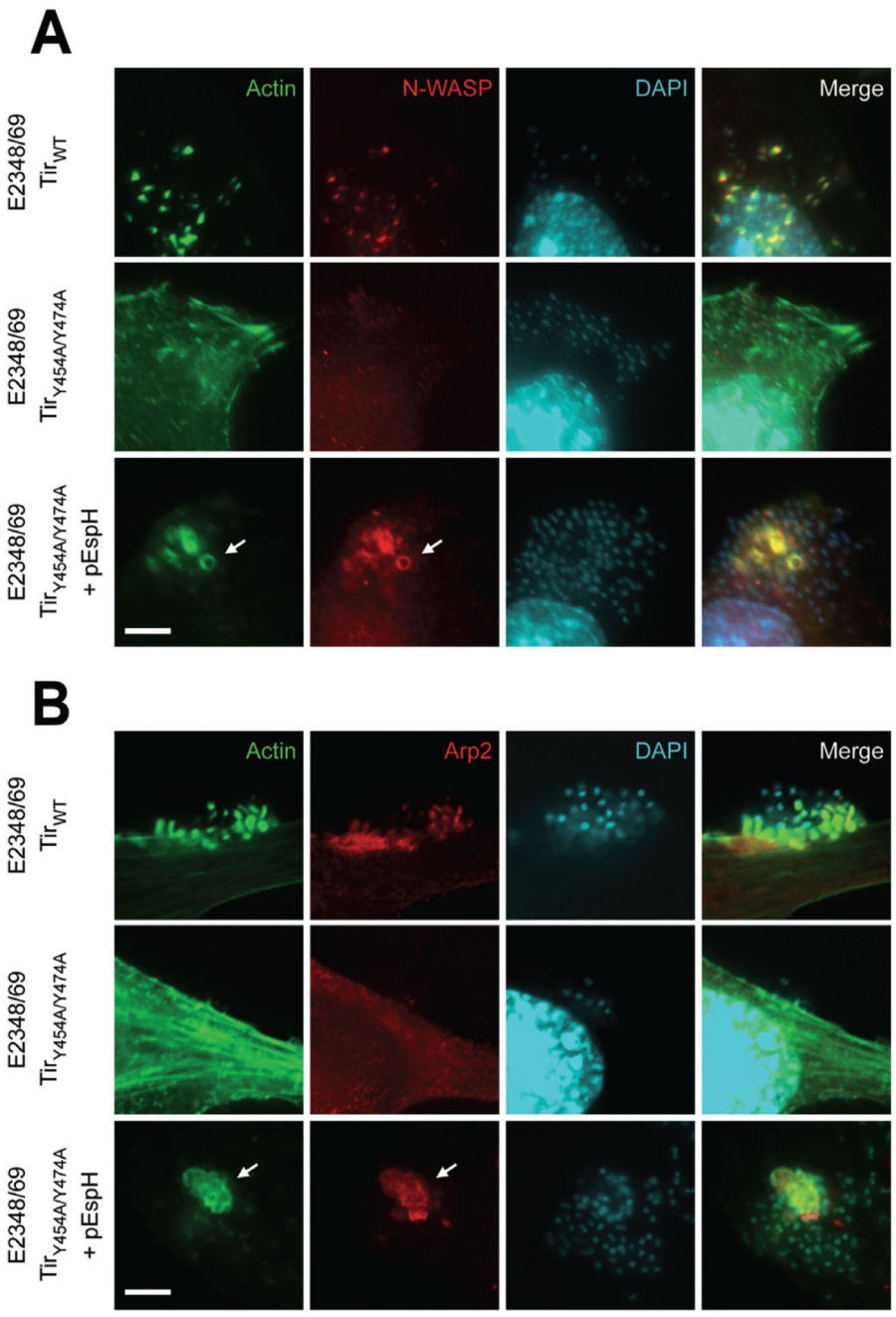

Fig. 2. EspH promotes recruitment of N-WASP and the Arp2 subunit of the Arp2/3 complex independently of Tir tyrosine residues Y454 and Y474.

Infection of Swiss 3T3 fibroblasts with E2348/69 expressing Tir_{WT}, $Tir_{Y454A/Y474A,}$ or coexpressing $Tir_{Y454A/Y474A}$ and EspH (E2348/69 $Tir_{Y454A/Y474A}$ + pEspH). N-WASP (A) or the Arp2/3 complex (B) was detected with anti-N-WASP antibody or anti-Arp2 antibody respectively (red). Actin was stained with Oregon green phalloidin (green), and bacteria were visualized with DAPI staining (cyan). N-WASP (A) and the Arp2 subunit (B) were both detected under adherent E2348/69 expressing Tir_{WT} and E2348/69 $Tir_{Y454A/Y474A}$ + pEspH (arrows), but not $Tir_{Y454A/Y474A}$ alone. Bar = 5 μm.

Europe PMC Funders Author Manuscripts

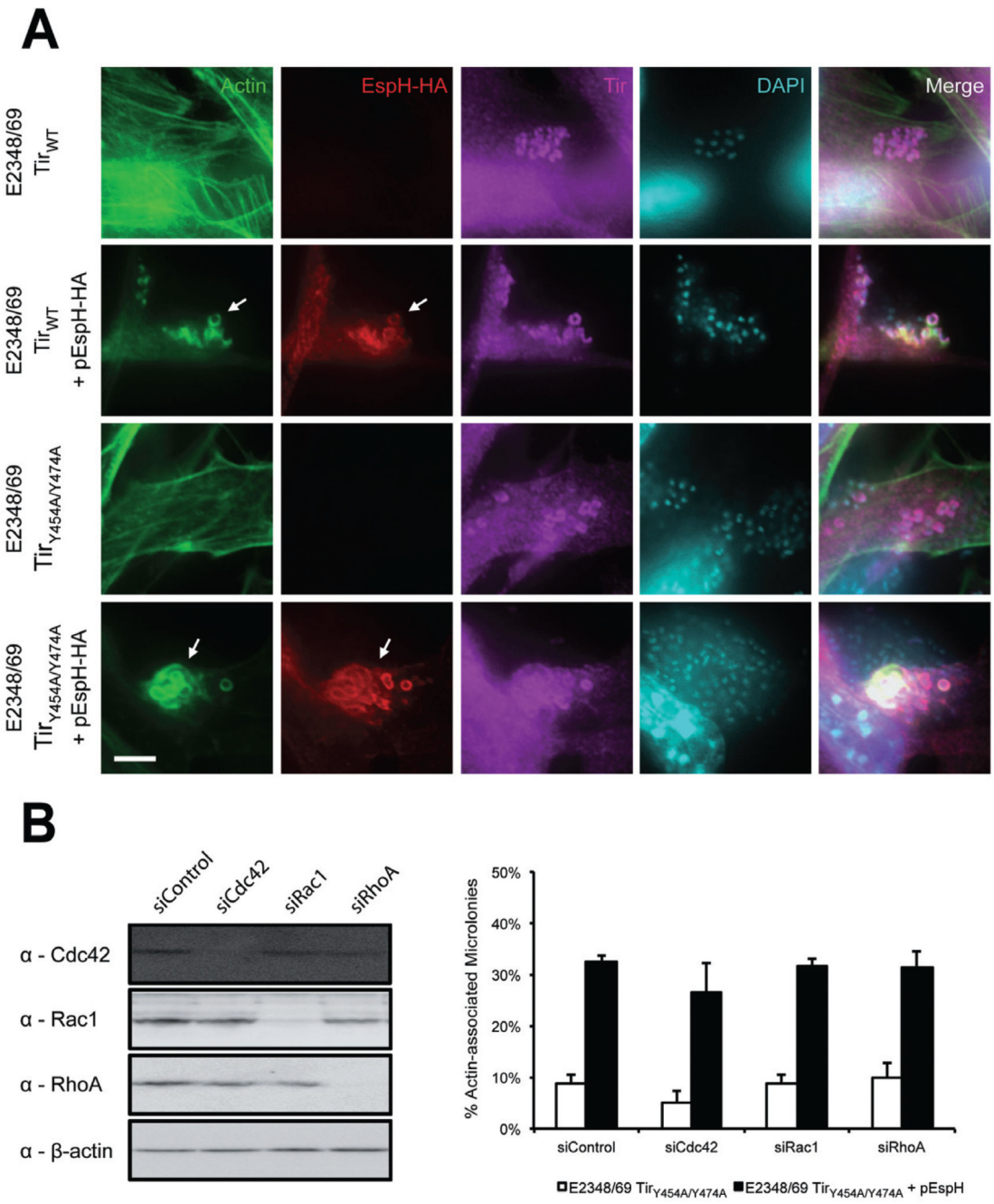

Fig. 3. Nck and Rho GTPases are not involved in EspH-mediated actin polymerization.

A. Infection of Nck-deficient (Nck$^{-/-}$) fibroblasts with E2348/69 Tir$_{WT}$ or E2348/69 Tir$_{Y454A/Y474A,}$ with or without pEspH-HA. Actin was stained with Oregon green phalloidin (green), HA-tagged EspH was detected with anti-HA antibody (red), Tir was detected with anti-Tir antibody (magenta) and bacteria were visualized with DAPI staining (cyan). Expression of EspH induced localized actin polymerization in both E2348/69 Tir$_{WT}$ and E2348/69 Tir$_{Y454A/Y474A}$ (arrows). Bar = 5 μm.

B. Immunoblotting of Swiss 3T3 fibroblasts treated with siRNA against Cdc42, Rac1 or RhoA. Scramble siRNA was used as a control (siControl). Specific RNAi-mediated silencing was detected with anti-Cdc42, anti-Rac1 or anti-RhoA antibodies, with β-actin used as loading control. Quantification of EPEC microcolonies associated with actin on siRNA-treated cells infected with E2348/69 expressing $Tir_{Y454A/Y474A,}$ with or without EspH (pEspH) revealed that the Rho GTPases play no role in formation of EspH-induced actin coats. A total of 100 microcolonies were counted in triplicates. Results are presented as a mean ± SD of three independent experiments.

Europe PMC Funders Author Manuscripts

Europe PMC Funders Author Manuscripts

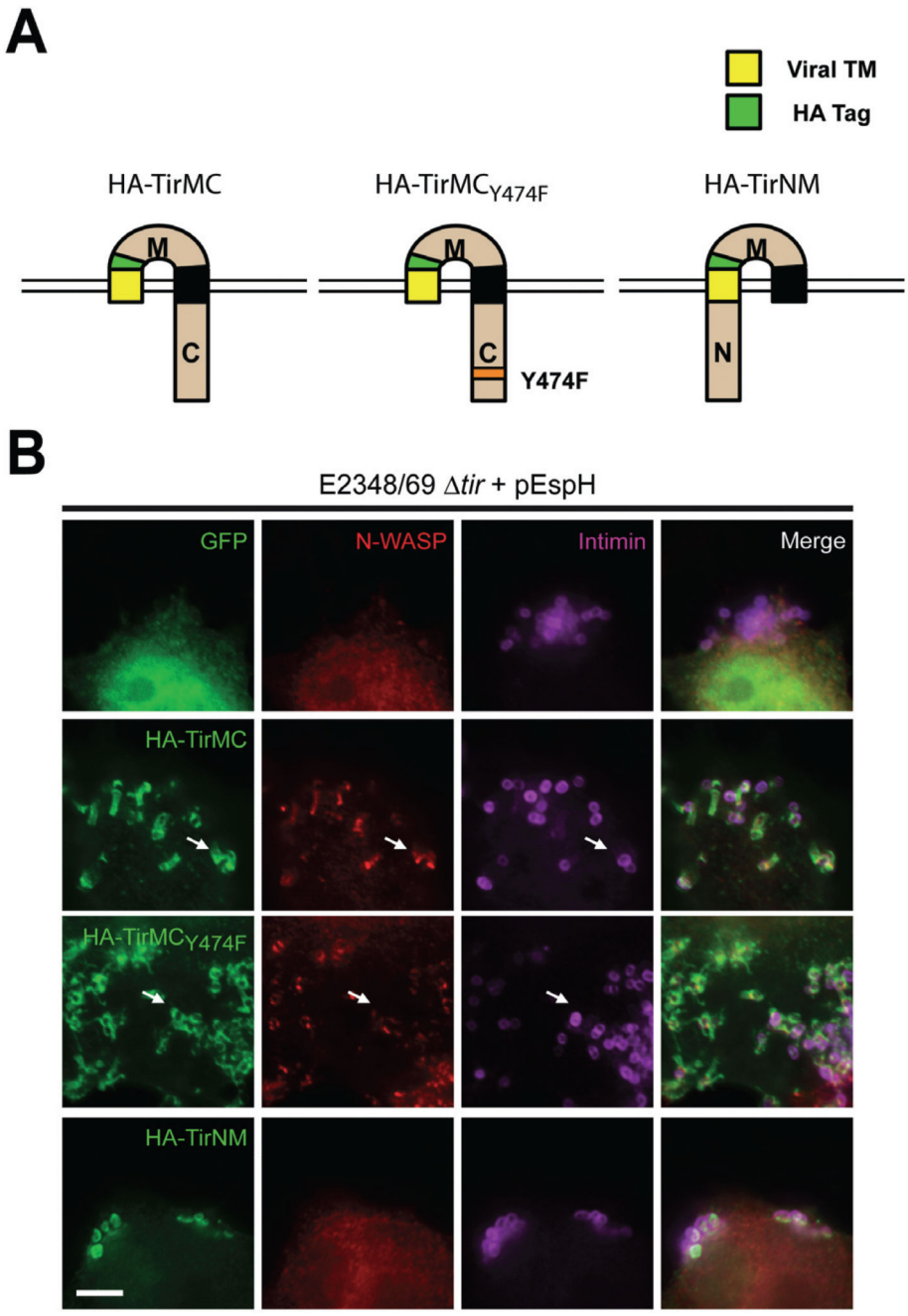

Fig. 4. EspH-mediated N-WASP recruitment is dependent on the C-terminus of Tir.

A. Schematic representation of Tir transfection derivatives comprising HA-TirMC, HA-TirMC$_{Y474F}$ and HA-TirNM.

B. Swiss 3T3 fibroblasts were transfected with the Tir derivatives, or GFP as negative control and infected with E2348/69Δ*tir* expressing EspH (E2348/69Δ*tir* + pEspH). HA-tagged Tir was detected with anti-HA antibody (green), N-WASP was detected with an anti-N-WASP antibody (red) and bacteria were visualized with an anti-intimin antibody (magenta) to indicate positive Tir clustering. N-WASP was not detected beneath adherent

microcolonies in cells transfected with GFP or HA-TirNM. Transfection of HA-TirMC or HA-TirMC$_{Y474F}$ complemented recruitment of N-WASP by E2348/69Δ*tir* + pEspH (arrows). Bar = 5 μm.

Europe PMC Funders Author Manuscripts

Europe PMC Funders Author Manuscripts

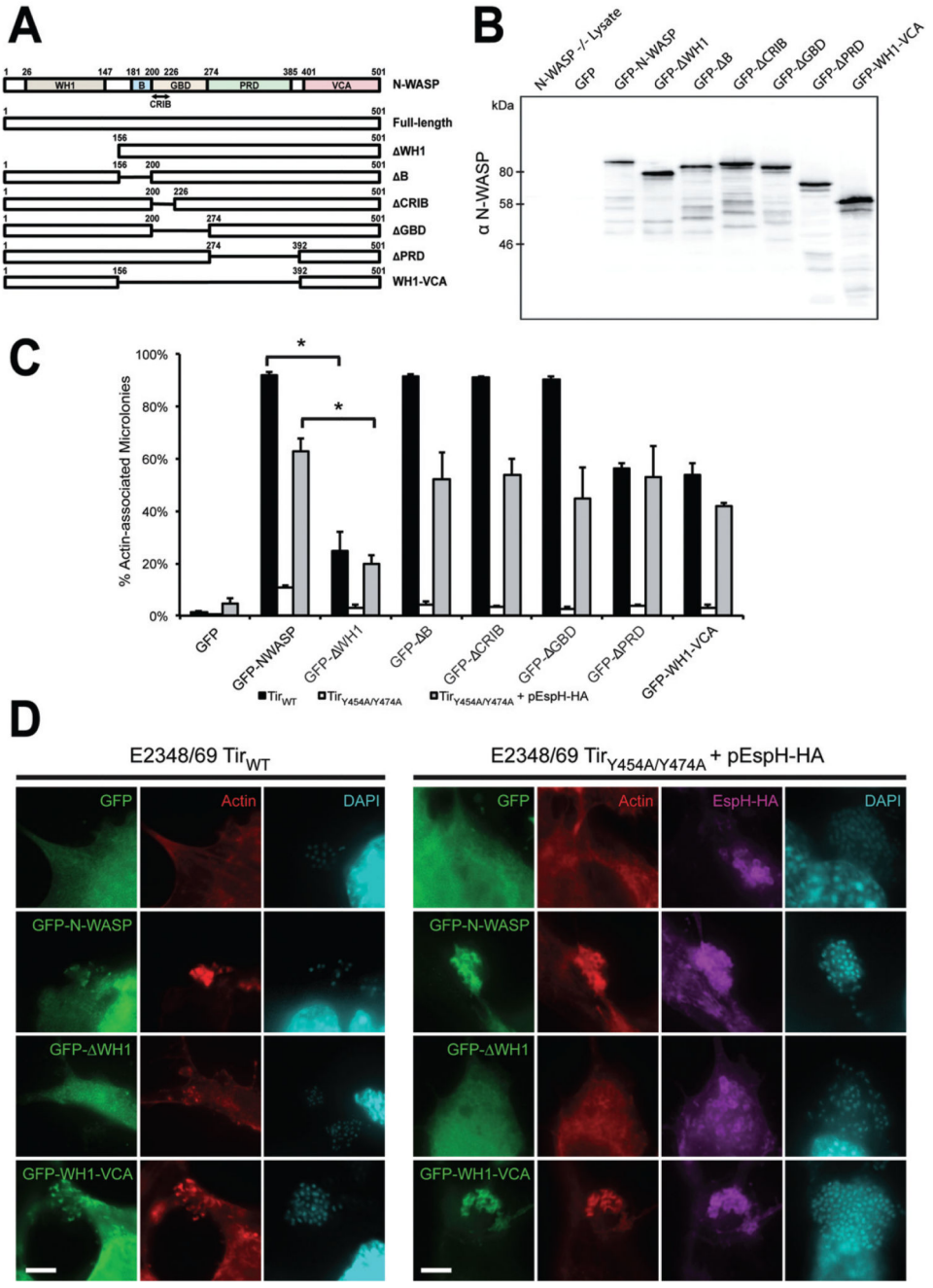

Fig. 5. EspH-mediated actin polymerization is dependent on the WH1 domain of N-WASP.

A. Schematic representation of N-WASP deletion variants GFP-ΔWH1, GFP-ΔB, GFP-ΔCRIB, GFP-ΔGBD, GFP-ΔPRD and GFP-WH1-VCA.

B. Lysates of N-WASP$^{-/-}$ mouse embryonic fibroblasts (MEFs) transfected with GFP or GFP-N-WASP deletion variants were immunoblotted and probed with anti-N-WASP antibodies. GFP-N-WASP was detected as a ~ 90 kDa protein; no N-WASP was detected on N-WASP$^{-/-}$ MEFs transfected with GFP alone. Ectopic expression of GFP-ΔWH1, GFP-ΔB,

GFP-ΔCRIB, GFP-ΔGBD, GFP-ΔPRD and GFP-WH1-VCA resulted in accumulation of intact fusion proteins.

C. Quantification of EPEC microcolonies associated with actin in N-WASP$^{-/-}$ MEFs expressing GFP-N-WASP deletion variants and infected with E2348/69 expressing Tir_{WT}, $Tir_{Y454A/Y474A,}$ or coexpressing $Tir_{Y454A/Y474A}$ and EspH-HA (E2348/69 $Tir_{Y454A/Y474A}$ + pEspH-HA). A total of 100 microcolonies were counted in triplicates. Results are presented as a mean ± SD of three independent experiments. Asterisks indicate statistical significance ($P < 0.001$).

D. N-WASP$^{-/-}$ MEFs transfected with different GFP-N-WASP deletion variants were infected with E2348/69 Tir_{WT} or E2348/69 $Tir_{Y454A/Y474A}$ + pEspH-HA. HA-tagged EspH was detected with anti-HA antibody (green), actin was stained with TRITC phalloidin (red) and bacteria were visualized with DAPI staining (cyan). No actin was detected beneath adherent microcolonies in GFP-transfected cells. Actin polymerization was significantly impaired in GFP-ΔWH1-transfected cells infected with either E2348/69 Tir_{WT} or $Tir_{Y454A/Y474A}$ + pEspH-HA. Transfection with GFP-WH1-VCA was sufficient to restore actin polymerization in E2348/69 Tir_{WT} and $Tir_{Y454A/Y474A}$ + pEspH-HA (arrow). Bar = 5 μm.

Europe PMC Funders Author Manuscripts

Europe PMC Funders Author Manuscripts

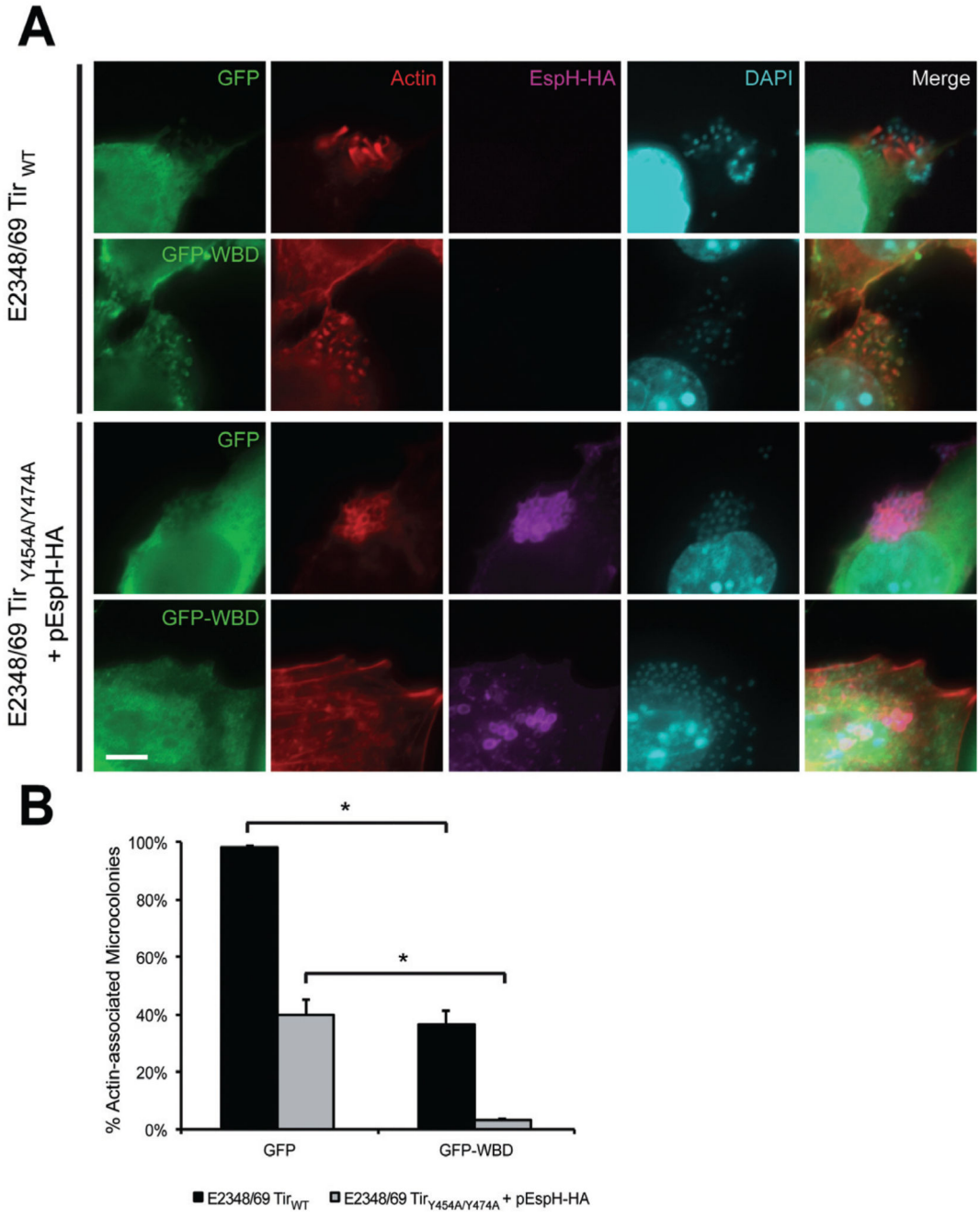

Fig. 6. Disruption of WIP/N-WASP binding abolishes EspH-mediated actin polymerization.

A. Swiss 3T3 fibroblasts transfected with GFP or GFP fused to the WASP binding domain of WIP (GFP-WBD), with infected with E2348/69 expressing Tir_{WT} or $Tir_{Y454A/Y474A}$ + pEspH-HA. Actin was stained with TRITC phalloidin (red), HA-tagged EspH was detected with anti-HA antibody (magenta), and bacteria were visualized with DAPI staining (cyan). Transfection with GFP-WBD diminished actin pedestal formation and elongation in E2348/69 Tir_{WT}, but completely abolishes EspH-mediated actin polymerization in $Tir_{Y454A/Y474A}$ + pEspH-HA (arrows). Bar = 5 μm.

B. Quantification of EPEC microcolonies associated with actin in transfected cells infected with E2348/69 Tir_{WT} or $Tir_{Y454A/Y474A}$ + pEspH-HA. A total of 100 microcolonies were counted in triplicates. Results are presented as a mean ± SD of three independent experiments. Asterisks indicate statistical significance ($P < 0.001$).

Europe PMC Funders Author Manuscripts

Europe PMC Funders Author Manuscripts

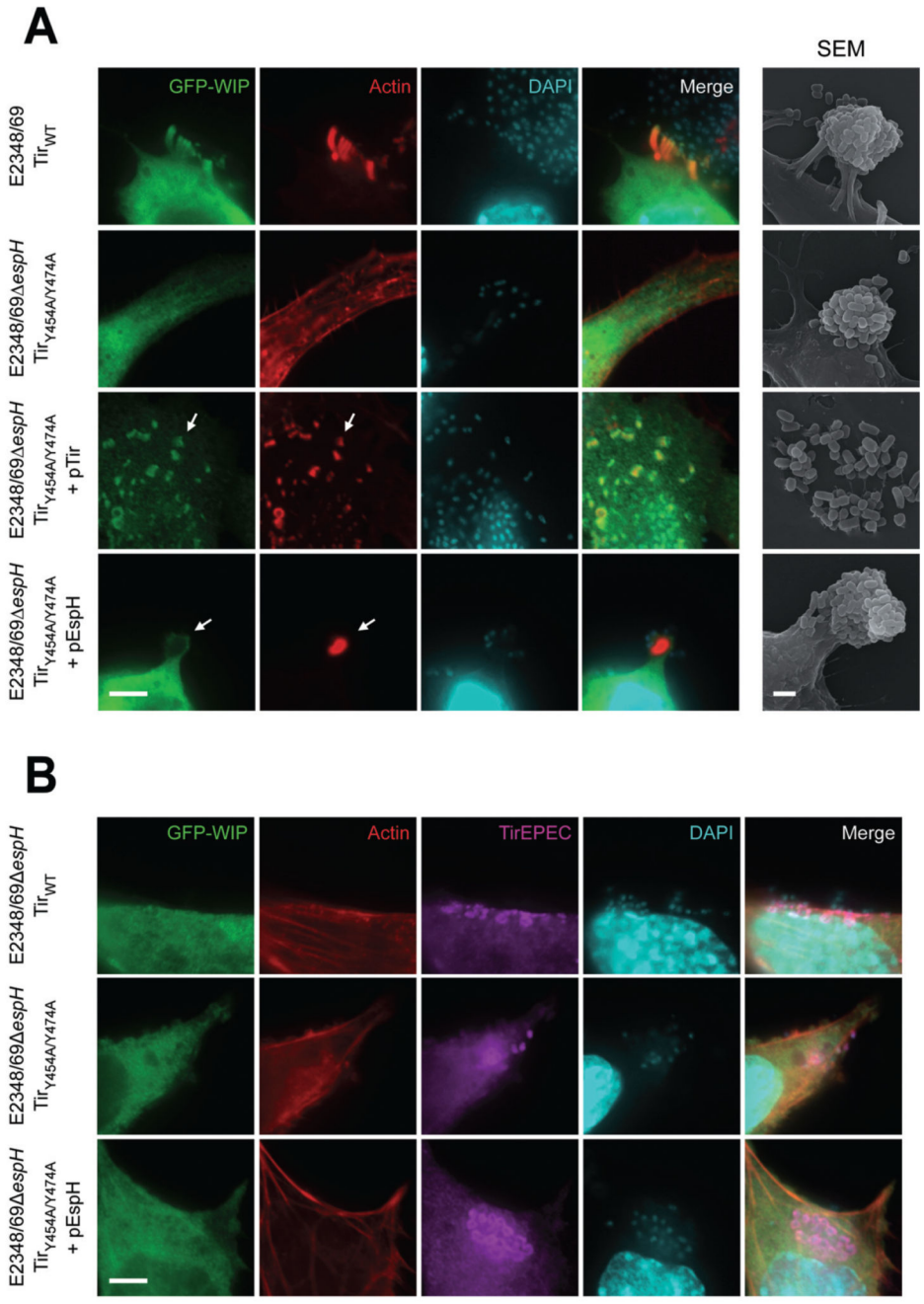

Fig. 7. Tir and EspH recruit WIP to EPEC attachment sites.

A. Swiss 3T3 fibroblasts transfected with GFP-WIP were infected with E2348/69 expressing Tir_{WT}, E2348/69Δ*espH* expressing $Tir_{Y454A/Y474A}$ or E2348/69Δ*espH* $Tir_{Y454A/Y474A}$ complemented with either plasmid-expressed Tir (pTir) or EspH (pEspH). Actin was stained with TRITC phalloidin (red), and bacteria were visualized with DAPI staining (cyan). WIP is recruited to the tip of the pedestal in cells infected with E2348/69 expressing Tir_{WT}, but not E2348/69Δ*espH* expressing $Tir_{Y454A/Y474A}$. Complementation of E2348/69Δ*espH* $Tir_{Y454A/Y474A}$ with either EPEC Tir or EspH restored the recruitment of WIP (arrows). Bar

= 5 μm. Scanning electron microscopy of the same experiment is displayed on the far right column (original magnification: ×6000). Bar = 2 μm.

B. Infection of N-WASP$^{-/-}$ MEFs transfected with GFP-WIP, with E2348/69 expressing Tir_{WT}, E2348/69Δ*espH* expressing $Tir_{Y454A/Y474A}$, or E2348/69Δ*espH* $Tir_{Y454A/Y474A}$ + pEspH. Tir was detected with anti-TirEPEC antibody (magenta), actin was stained with TRITC phalloidin (red), and bacteria were visualized with DAPI staining (cyan). Both E2348/69 Tir_{WT} and E2348/69Δ*espH* $Tir_{Y454A/Y474A}$ + pEspH were unable to recruit WIP or trigger actin polymerization. Bar = 5 μm.

Europe PMC Funders Author Manuscripts

Europe PMC Funders Author Manuscripts

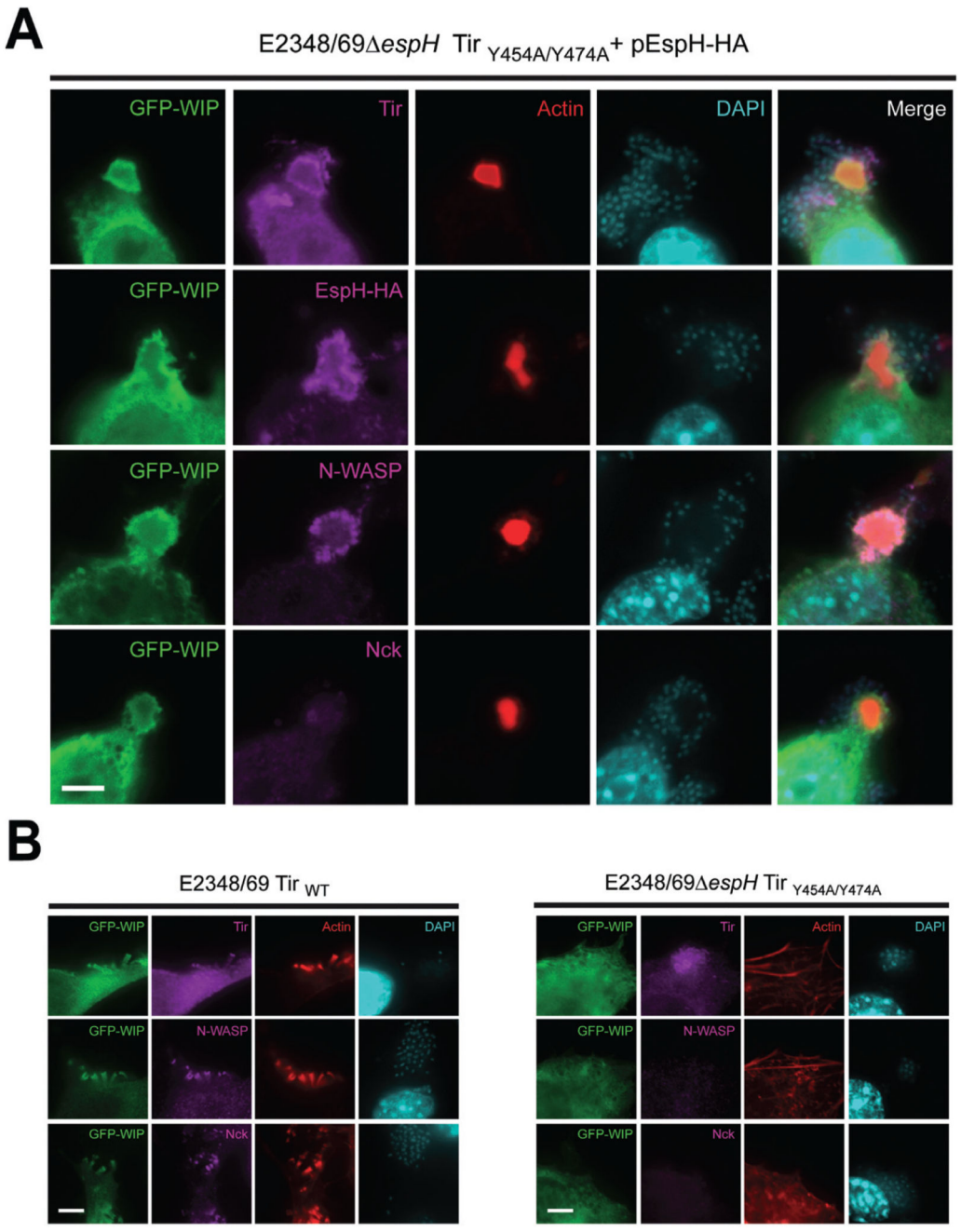

Fig. 8. EspH induces colocalization of Tir, WIP and N-WASP, but not Nck.

A. Swiss 3T3 fibroblasts transfected with GFP-WIP were infected with E2348/69Δ*espH* coexpressing $Tir_{Y454A/Y474A}$ and HA-tagged EspH (E2348/69Δ*espH* $Tir_{Y454A/Y474A}$ + pEspH-HA). Tir, EspH-HA, N-WASP and Nck were labelled with respective antibodies (magenta), actin was stained with TRITC phalloidin (red), and bacteria were visualized with DAPI staining (cyan). Tir, EspH and N-WASP colocalized with WIP, but not Nck. Bar = 5 μm.

B. Swiss 3T3 fibroblasts transfected with GFP-WIP were infected with E2348/69 expressing Tir_{WT}, or E2348/69Δ*espH* expressing $Tir_{Y454A/Y474A}$. Tir, N-WASP, and Nck were labelled with respective antibodies (magenta), actin was stained with TRITC phalloidin (red), and bacteria were visualized with DAPI staining (cyan). Tir, Nck and N-WASP colocalizes with WIP at the tip of actin pedestals in E2348/69 Tir_{WT}. Bar = 5 μm.

Europe PMC Funders Author Manuscripts

Europe PMC Funders Author Manuscripts

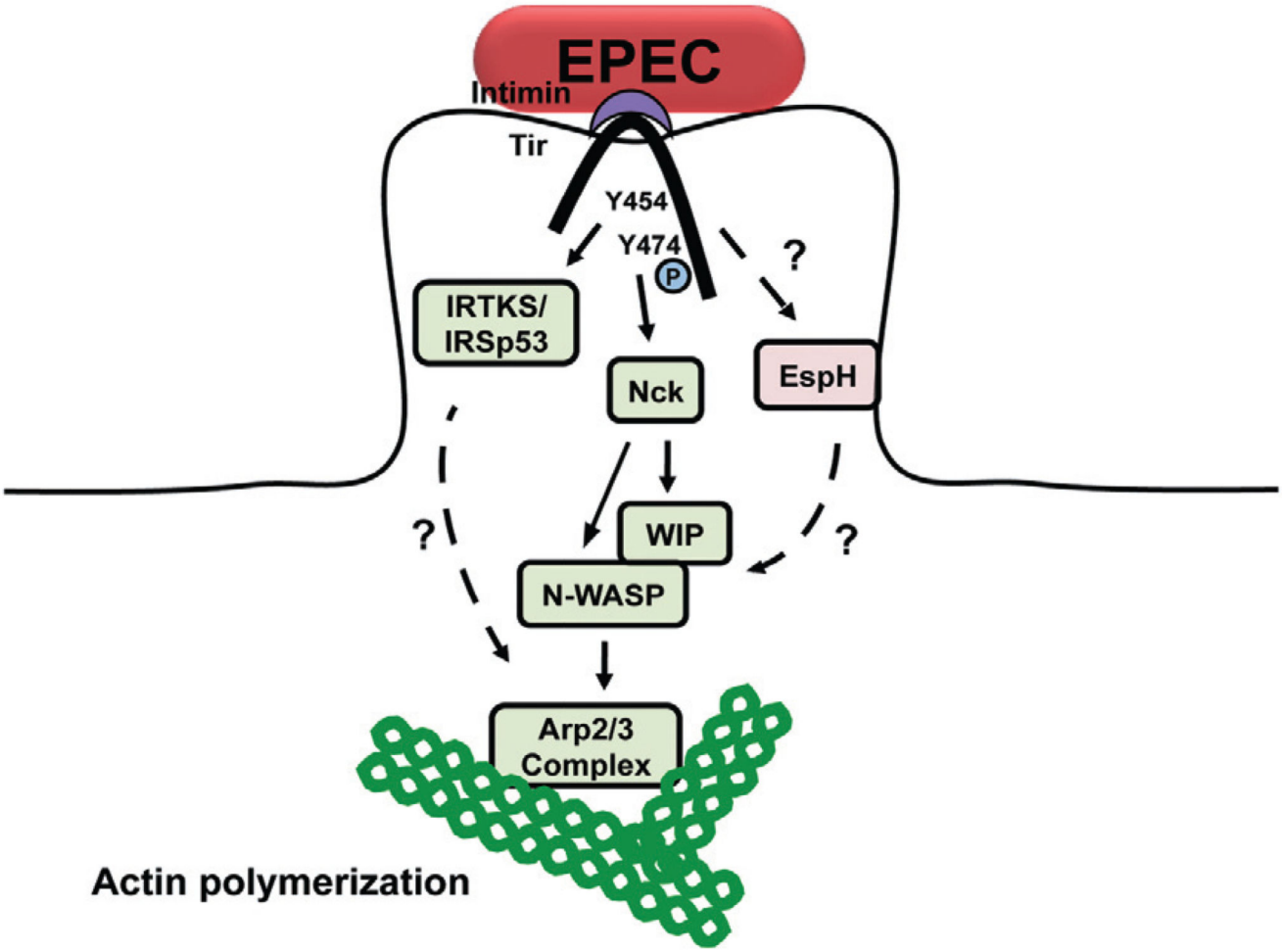

Fig. 9. EPEC induces distinctive, convergent and synergistic Tir actin signalling cascades.

A model for Tir-mediated actin signalling cascades. Upon translocation, Tir inserts into the plasma membrane, where clustering with the bacterial adhesion intimin initiates several actin signalling pathways. Phosphorylation at Y474 leads to Nck binding. Nck, which binds both WIP and N-WASP, then induces actin pedestal formation. Y454 forms part of an NPY motif that binds IRTKS/IRSp53 to induce weak actin polymerization, although the mechanism remains unknown. In addition, EspH is recruited via the C-terminus of Tir to the bacterial attachment site where the effector, directly or indirectly, promotes WIP and N-WASP recruitment independently of Nck or Y454/Y474 to promote formation and elongation of EPEC actin pedestals.

Europe PMC Funders Author Manuscripts

Table 1

List of strains.

ICC No.	Name	Description	Source/reference
	E2348/69	Wild-type EPEC 1 O127:H6 strain	Levine *et al.* (1978)
ICC225	E2348/69Δ*tir*	E2348/69 *tir* deletion mutant	Berger *et al.* (2009)
ICC308	E2348/69 Tir_{WT}	Control for Tir chromosomal mutants (with kanamycin cassette)	This study
ICC309	E2348/69 Tir_{Y454A}	E2348/69 chromosomal mutant expressing Tir_{Y454A}	This study
ICC310	E2348/69 Tir_{Y474A}	E2348/69 chromosomal mutant expressing Tir_{Y474A}	This study
ICC311	E2348/69 $Tir_{Y454A/Y474A}$	E2348/69 chromosomal mutant expressing $Tir_{Y454A/Y474A}$	This study
ICC312	E2348/69Δ*espH* $Tir_{Y454A/Y474A}$	E2348/69 chromosomal mutant expressing $Tir_{Y454A/Y474A}$, with *espH* deletion	This study

Table 2

List of plasmids.

pICC No.	Plasmids	Description	Source/reference
	pSA10	pKK177-3 containing *lacI* gene	Levine *et al.* (1978)
	pGEMT	Cloning vector	Promega
	pKD46	Coding the lambda-red recombinase	Datsenko and Wanner (2000)
	pSB315	Coding the kanamycin resistance *aphT* cassette	Galan *et al.* (1992)
pICC618	PSB315-CM	pSB315 with chloramphenicol resistance *cat* cassette replacing the *aphT* cassette	This study
pICC619	pSA10-EspH	pSA10 derivative encoding EPEC EspH	This study
pICC394	pSA10-Tir	pSA10 derivative encoding EPEC Tir	Berger *et al.* (2009)
pICC528	pSA10-EspH-HA	pSA10 derivative encoding haemagglutinin (HA)-tagged EspH	This study
pICC530		pGEMT vector containing 3′ end of tir_{EPEC} (bp 1072–1653), *aphT, tir-cesT* intergenic region and 5′ end of *cesT* (bp 1–369)	This study
pICC531		pICC530 containing the tir_{EPEC} Y454A mutation	This study
pICC532		pICC530 containing the tir_{EPEC} Y474A mutation	This study
pICC533		pICC530 containing the tir_{EPEC} Y454A/Y474A mutation	This study
	pEGFP-C1	Coding a GFPmut1 variant for expression in mammalian cells	Invitrogen
	pEGFP-N-WASP	pEGFP-C1 derivative encoding N-WASP	E. Caron
pICC620	pEGFP-ΔWH1	pEGFP-N-WASP with aa 1–156 deletion	This study
pICC621	pEGFP-ΔB	pEGFP-N-WASP with aa 156–200 deletion	This study
pICC622	pEGFP-ΔCRIB	pEGFP-N-WASP with aa 200–226 deletion	This study
pICC623	pEGFP-ΔGBD	pEGFP-N-WASP with aa 200–274 deletion	This study
pICC624	pEGFP-ΔPRD	pEGFP-N-WASP with aa 274–385 deletion	This study
pICC625	pEGFP-WH1-VCA	pEGFP-N-WASP with aa 156–385 deletion	This study
	pCB6-WIP	GFP fused to WIP transfection vector	Moreau *et al.* (2000)
	pCB6-WBD	GFP fused to WASP-binding domain of WIP transfection vector	Moreau *et al.* (2000)
	pRK5myc-IRSp53	Myc-tagged IRSp53 construct	Millard *et al.* (2007)
	pRK5myc-WAVE2	Myc-tagged WAVE2 construct	L. Machesky
	pCDNA3-TirMC	HA-tagged Tir derivative	Campellone *et al.* (2004a)
	pCDNA3-TirMCY$_{474}$	HA-tagged Tir derivative	Campellone *et al.* (2004a)
pICC626	pCDNA3-TirNMC	pCDNA3-TirMC with Tir N-terminus (aa 1–233) insertion at the HindIII restriction site	This study
pICC627	pCDNA3-TirNM	pCDNA-TirNMC with aa 388–547 deletion	This study
pICC628		pGEMT vector containing 325 bp upstream region of $espH_{EPEC}$, *cat*, and 499 bp downstream region of $espH_{EPEC}$	This study

Table 3

List of primers.

Name	Nulceotide sequence (5′–3′) (restriction sites in bold)
EcoRI-EspH-E69-Fw	CGG**GAATTC**ATGTCGTCATCATTATCAGGTATAAC
PstI-EspH-E69-Rv	AAAA**CTGCAG**TTAAACTGTCACACCTGATAAAG
PstI-EspH-E69-HA-Rv	AAAA**CTGCAG**TTATGCGTAATCTGGTACATCGTATGGGTATGCTCCAA CTGTCACACCTGATAAAGAGTTTAATG
EPEC *tir* mutagenesis	
TirC-E69-Fw	TACAGCTTTCATCGGGTATTGG
EcoRI-TirC-E69-Rv	CGG**GAATTC**TTAAACGAAACGTACTGGTCCC
EcoRI-NcesT-E69-Fw	CGG**GAATTC**ATATATCTGTGAGTATTTAGTTGAG
NcesT-E69-Rv	CGTTAAGTCGATGGAAAATCTG
TirC-E69-Y454A-Rv	GGCAGGATTAACCACTTCGCTAGA
TirC-E69-Y454A-Fw	GCTGAAGTTGGGGGGGCTC
TirC-E69-Y474A-Rv	GGCTATATGCTCTTCTGGCTGATG
TirC-E69-Y474A-Fw	GATGAGGTCGCTGCAGATCCT
EPEC *espH* mutagenesis	
Up-EspH-E69-Fw	GGCAACCGTAAAGCTGAGC
BamHI-Up-EspH-E69-Rv	CGC**GGATCC**CATACACCTCCCTATATAACG
BamHI-Dn-EspH-E69-Fw	CGC**GGATCC**CTCTTTATCAGGTGTGACAG
Dn-EspH-E69-Rv	GTCATGAGTGGATACTTGAG
GFP-N-WASP variants	
NWASP-WH1del-Rv	CATGGTGTCGCCGGACTTG
NWASP-WH1del-Fw	GCTACAGTTGACATAAAAAATCC
NWASP-Bdel-Rv	CATGGGTAGATTGGGACCATT
NWASP-Bdel-Fw	GGAACACCAAGTAATTTCCAGC
NWASP-CRIBdel-Rv	AATATCTGCCTTGGTTAATCTCTTC
NWASP-CRIBdel-Fw	CCAGAATTAAAGAATCTTTTTGATATG
NWASP-GBDdel-Fw	CCACCACCTCCACCCTCGAG
NWASP-PRDdel-Rv	TGGTGCTTGTCTTCGGAGTTC
NWASP-PRDdel-Fw	CATCAAGTTCCAGCTCCTTCAG
HA-TirNM	
HindIII-TirN(1–233)-E69-Fw	CCC**AAGCTT**CAATGCCTATTGGTAACCTTGGTAAT
HindIII-TirN(1–233)-E69-Rv	CCC**AAGCTT**GTTTAGGATCTGAGCGAACGCTG
pCDNA3-TirNM(EPEC)-Rv	TCTATGGAGCGCAGTCGTTAC
pCDNA3-TirNM(EPEC)-Fw	CGTTTCGTTTAAATATATCCGCG